eNeuro

Research Article: New Research | Disorders of the Nervous System

Distinct aging-vulnerable and -resilient trajectories of specific motor circuit functions in oxidation- and temperature-stressed *Drosophila*

https://doi.org/10.1523/ENEURO.0443-21.2021

Cite as: eNeuro 2021; 10.1523/ENEURO.0443-21.2021

Received: 18 October 2021
Revised: 2 November 2021
Accepted: 5 November 2021

Title:
Distinct aging-vulnerable and -resilient trajectories of specific motor circuit functions in oxidation- and temperature-stressed *Drosophila*

Abbreviated Title:
Aging-vulnerable and -resilient motor circuit properties

Authors:
Atulya Iyengar[1, 2, 3,†], Hongyu Ruan[1, *, †], and Chun-Fang Wu[1, 2, 3]

[1]Department of Biology, University of Iowa, Iowa City, IA 52242, USA. [2]Iowa Neuroscience Institute, University of Iowa, Iowa City, IA 52242, USA. [3]Interdisciplinary Graduate Program in Neuroscience, University of Iowa, Iowa City, IA 52242, USA.
[*]Present Affiliation: Department of Psychiatry, SUNY Upstate Medical University, Syracuse, NY 13210
[†] Equal contributions

Author Contributions: AI, HYR, CFW designed research; AI, HYR performed research; AI, HYR, CFW analyzed data; AI, HYR, CFW wrote the paper.

Address correspondence to:
Prof. Chun-Fang Wu
Department of Biology
University of Iowa
Iowa City, IA 52242
Telephone number: (319) 335-1090
Email: chun-fang-wu@uiowa.edu

Manuscript Information:
Number of Figures: 7 (3 extended data figures); Number of Tables: 1; Number of Multimedia: 0; Abstract: 219 words; Significance statement: 120; Introduction: 612; Discussion: 3107 words

Acknowledgements:
We thank Xiaomin Xing, Scott Woods, Tristan O'Harrow and Atsushi Ueda for critical discussions during the projects, Jeff Nirschl, Jordan Imoehl, Kelle Goranson, and Amy Hoehne for assistance in data collection.

Conflict of Interest:
The authors declare that no conflict of interest exists.

Funding Sources:
This research was supported by a University of Iowa Biological Sciences Funding Program Grant and NIH grants, GM088804 AG047612, and AG051513 to CFW; and by an NIH Pre-Doctoral NRSA NS082001 and Iowa Neuroscience Institute Post-Doctoral Fellowships to AI

Title:
Distinct aging-vulnerable and -resilient trajectories of specific motor circuit functions in oxidation- and temperature-stressed *Drosophila*

Abstract

In *Drosophila*, molecular pathways affecting longevity have been extensively studied. However, corresponding neurophysiological changes underlying aging-related functional and behavioral deteriorations remain to be fully explored. We examined different motor circuits in *Drosophila* across the lifespan and uncovered distinctive age-resilient and age-vulnerable trajectories in their established functional properties. In the giant-fiber (GF) and downstream circuit elements responsible for the jump-and-flight escape reflex, we observed relatively mild deterioration toward the end of lifespan. In contrast, more substantial age-dependent modifications were seen in the plasticity of GF afferent processing, specifically in use-dependence and habituation properties. In addition, there were profound changes in different afferent circuits that drive flight motoneuron activities, including flight pattern generation and seizure spike discharges evoked by electroconvulsive stimulation. Importantly, in high temperature (HT)-reared flies (29 ℃), the general trends in these age-dependent trajectories were largely maintained, albeit over a compressed time scale, lending support for the common practice of HT rearing for expediting *Drosophila* aging studies. We discovered that shortened lifespans in *Cu/Zn superoxide dismutase* (*Sod*) mutant flies were accompanied by altered aging trajectories in motor circuit properties distinct from those in HT-reared flies, highlighting differential effects of oxidative vs temperature stressors. This work helps to identify several age-vulnerable neurophysiological parameters that may serve as quantitative indicators for assessing genetic and environmental influences on aging progression in *Drosophila*.

Significance statement

Comparisons of the aging trajectories of performance changes of several motor circuits in *Drosophila* revealed remarkably heterogeneous age-progressions. We identified “aging-resilient” and “aging-vulnerable” circuits in both normal control and flies with shortened lifespans due to either elevated rearing temperature or oxidative stress. Motor circuit components including flight motor neuron and the giant-fiber pathway responsible for the escape reflex showed only mild functional decline, whereas distinct trajectories throughout lifespan were seen in the flight

pattern generator, interneuron inputs to the giant-fiber system, and circuits generating seizure discharge patterns. Notably, high-temperature rearing generally compressed aging trajectories while *Sod* mutation-induced oxidative stress led to distinct patterns of motor defects. Together, these results elucidate potentially salient neurophysiological markers for aging in flies.

Introduction

Aging nervous systems manifest a progressive functional decline. Invertebrate preparations offer experimentally tractable, simpler nervous systems with individually identifiable neurons to reveal the molecular and cellular bases of age-related neurophysiological changes (Atwood, 1992; Janse et al., 1986; Kenyon, 2001; Pletcher et al., 2002; Toivonen & Partridge, 2009; Yeoman & Faragher, 2001). In *Drosophila*, characteristic declines over the lifespan have been documented in motor coordination (Gargano et al., 2005; Leffelaar & Grigliatti, 1983) and in higher functions, such as learning and memory (Tamura et al., 2003; Yamazaki et al., 2007). However, fewer studies have directly assessed cellular physiological decline underlying changes in behavioral performance across the lifespan (Banerjee et al., 2021; Martinez et al., 2007). It is important, therefore, to identify the neural circuits and associated behavioral outputs that are prone to age-related modifications and determine whether specific neuronal elements are differentially vulnerable in this process. Given that environmental and genetic contributions must be both considered in studies of the aging process (Curtsinger et al., 1995; Mair et al., 2003; Miquel et al., 1976), it is equally important to examine how age-progression of circuit function is differentially modified by extrinsic environmental and intrinsic genetic factors. Such analyses may also uncover salient physiological parameters suitable for the assessment of aging progression.

This study examines several motor-pattern circuits in *Drosophila* whose outputs converge on a small subset of identified, well-described, flight motor neurons that innervate the indirect flight muscles (dorsal longitudinal muscles, DLM a-f, each receiving input from a single motor neuron, see Levine, 1973). Thus the DLM readout, driven by different motor circuits, enabled us to determine how age-dependent changes in different categories of motor performance are modified by either high-temperature rearing (29 ˚C, leading to a shortened lifespan), or oxidative stress in short-lived *Cu/Zn Superoxide dismutase* (*Sod*) mutants (defective in a major free radical-scavenging enzyme, see Campbell et al., 1986; Phillips et al., 1989). Rearing flies at 29 ˚C is a widely adopted protocol for experimental expedience in *Drosophila* aging and neurodegeneration studies (e.g. Biteau et al., 2010; Kang et al., 2002; Min & Benzer, 1997; Simon et al., 2003; Sudmeier et al., 2015). Our study directly investigated the impact of rearing at 29 ˚C on different motor functions over the lifespan, as well as the cellular physiological links between proposed oxidative stress mechanisms (Finkel & Holbrook, 2000; Harman, 1956;

Ziegler et al., 2015) and the associated behavioral alterations previously described for *Sod* mutant flies.

We also present an overall assessment of the trajectory of neural circuit performance associated with different categories of motor behaviors along normal and altered lifespans. These include flight pattern generation (Harcombe & Wyman, 1977; Levine, 1973) the giant fiber (GF) pathway-mediated jump and flight escape reflex (Engel & Wu, 1992; Gorczyca & Hall, 1984; Tanouye & Wyman, 1980), habituation of the GF pathway escape response to repetitive stimulation (a form of non-associative learning, Engel & Wu, 1996; Engel et al., 2000) and a stereotypic seizure repertoire triggered by electroconvulsive stimulation (ECS, Kuebler & Tanouye, 2000; Lee et al., 2019; Lee & Wu, 2002, 2006; Pavlidis & Tanouye, 1995). Our analysis has identified age-resilient and age-sensitive circuit properties that are attributable to changes in distinct circuit components. Furthermore, we found WT flies reared at 29 °C manifested accelerated trajectories of age-dependent alterations resembling those at 25 °C at a normalized timescale, while *Sod* mutants displayed distinctively altered pattern of aging progression. Our findings also identify several neurophysiological parameters that could serve as quantitative indices for assessing age-related functional decline. These findings have been reported in part in PhD dissertations (Iyengar, 2016; Ruan, 2008) and in abstract form (Iyengar et al., 2010; Ruan & Wu, 2009; Wu & Ruan, 2008).

Methods

Fly Stock Maintenance and Lifespan Assays

The *Canton-S* wild-type (WT) strain and *Sod* mutant allele Sod^{1} were maintained on standard cornmeal medium (Frankel & Brousseau, 1968). Originally isolated in an EMS mutagenesis screen as *l-108* (Campbell et al., 1986), the Sod^{1} allele (also known as Sod^{n108}) was recombined on a *red* chromosome background (Phillips et al., 1989), and kept as a balanced stock Sod^{1} *red*/ TM3, *Sb Ser*. Among *Sod* alleles previously studied (e.g. Sod^{x39}, Sod^{n58}, Sod^{n64} all on the *red* background, Sod^{21} on a *white* background), Sod^{1} was selected for this study because this allele has been well characterized and could be more readily managed to generated sufficient numbers of flies for cross-sectional comparisons across the lifespan (Ruan & Wu, 2008; Şahin et al., 2017). For collecting rare homozygous offspring of *Sod* flies, the stock was grown in half-pint bottles to encourage reproduction. Newly eclosed adults were collected under

CO_2 anesthesia (WT every 1-2 days, *Sod* flies every 2 days) to assemble sufficient sample sizes to initiate lifespan assays. Flies were distributed into food vials (10-14 flies per vial for WT, 7-10 flies for *Sod*) and were transferred to fresh vials every 2 days. All vials were pre-warmed to the corresponding temperature before fly transfers. Foam plugs were used and the vials were kept horizontally to avoid weaker flies being accidentally stuck to food or cotton plugs. Flies were maintained in incubators set at 25 ˚C and 29 ˚C or 23 ˚C, were kept at the ambient humidity range of ~30 – 70%, and under 12:12 h light:dark conditions. Survivors were counted and dead flies were removed daily. When reported as a function of % mortality, flies were sampled within one day of the age corresponding with % mortality (see Results and Figure 1A).

Flight Assessment and Indirect Flight Muscle Recording

Preparation, stimulation, recording, and analysis of dorsal longitudinal muscle (DLM) responses have been described previously (Engel & Wu, 1992; Iyengar & Wu, 2014; Lee & Wu, 2002). Flies were anesthetized briefly on ice or by light ether exposure and glued to a metal wire between the head and thorax using a nitrocellulose or cyanoacrylate based adhesive (Gorczyca & Hall, 1984). Mounted flies were allowed at least 30 min rest in a humid chamber before recording. All electrophysiological and behavioral experiments were carried out at room temperature (21 - 23 ˚C).

Flights were triggered via a gentle 500 ms air puff generated by an aquarium air pump (Whisper 10-30 Tetra, Blacksburg, VA, USA) pumping air through a 4 mm diameter tube placed approximately 4 mm away from the fly. A 3-way solenoid valve (ASCO scientific, P/N AL4312, Florham Park, NJ, USA) driven by a USB 6210 DAQ card (National Instruments, Austin TX) controlled air flow. Wing sounds were picked up by a high-gain microphone placed approximately 4 mm below the fly. Acoustic signals were digitized by a PC sound card controlled by a LabVIEW 8.6 script. The wing beat frequency was determined using the short-time FFT procedure described in Iyengar & Wu (2014).

Action potentials from the top-most dorsal longitudinal muscle (#45a, Miller, 1950) were recorded by an electrolytically sharpened tungsten electrode penetrating the flight muscle with a similarly constructed electrode inserted in the abdomen for reference. Signals were accessed with an AC amplifier (Microelectrode AC Amplifier, Model 1800, A-M Systems, Inc., Carlsborg, WA; filter bandwidth from 10 Hz to 20 kHz). Amplified signals were recorded with pulse code

modulation (Neuro-Corder DR-484, Cygnus Technology, Inc., Delaware Water Gap, PA) on videotape at a sampling rate of 44 kHz. Digitization of spiking traces (Figures 1, 6 and Figure 5-1) was carried out by a digital acquisition card (USB 6210) controlled by custom-written LabVIEW scripts.

Giant Fiber Pathway Stimulation

As previously described (Engel & Wu, 1996), a pair of uninsulated tungsten electrodes were inserted in the eyes (anode in left eye) to pass stimulation of 0.1 ms duration (Isolated Pulse Stimulator, Model 2100, A-M Systems, Inc., Carlsborg, WA). Long-latency and short-latency response (LLR and SLR) thresholds were first determined using increasing stimulation intensity with an inter-stimulus interval of 30 s. For the experiments involving LLR (twin-pulse refractory period and habituation), stimulus intensity was set at least 0.5 V below the SLR threshold. For SLR-related trials, stimulus intensity was set at 20 V, which was well above the SLR thresholds in all flies tested (see Engel and Wu, 1992 for details).

To determine the refractory period of LLR and SLR, twin-pulse stimuli were given every 10 s, with the stimulus interval decreasing stepwise (step size: 5 - 10 ms for LLR, 0.5 - 1 ms for SLR) from a starting interval (100 - 800 ms for LLR, 10 - 20 ms for SLR). When a given inter-stimulus interval failed to trigger a second DLM spike in one or two trials, a 3 - 5 min rest was allowed before a train of six twin-pulses of the same inter-stimulus interval were delivered at 0.1 Hz between twin pulses. If all six trials failed, then the previous stimulus interval was recorded as the refractory period.

The ability of GF to follow high-frequency stimulation was determined as described previously (Engel & Wu, 1992; Gorczyca & Hall, 1984). Three trains of 10 pulses at 200 Hz with 10 s in between were delivered and the number of responses was counted.

Habituation of GF-Mediated LLRs and Electroconvlusive Stimulation-Evoked Seizures

For testing habituation rate, two trials of 100-pulse LLR stimulation trains at a given frequency (1, 2, and 5 Hz) were delivered with a 10 min interval between trials. The criterion for reaching habituation was the occurrence of the first five consecutive LLR failures (F5F, Engel & Wu, 1996). The larger F5F value of the two trials was recorded for the fly tested. Upon

reaching habituation criterion, an air puff dishabituation stimulus was delivered to confirm habituation (see Engel and Wu, 1996 for additional details).

High-frequency electroconvulsive stimulation (0.1-msec pulses at 200 Hz for 2 s at a particular voltage 15 - 80 V) were delivered across the brain to induce a stereotypic electroconvulsive seizure (ECS) discharge pattern (see Lee and Wu, 2002 for details). After high-frequency stimulation, test pulses of 20 volts or higher were sometimes delivered at 1 Hz to examine the failure and recovery of the GF pathway motor response. An interval of at least 10 min was allowed between each ECS to avoid the effect of refractoriness (Lee & Wu, 2002). For follow-up experiments of DLM spike patterning during ECS discharges (Figure 6 and Figure 5-1), spikes were detected and their timing recorded using custom-written Matlab scripts (Iyengar & Wu, 2014; Lee et al., 2019). Firing rate was measured by the instantaneous firing frequency (ISI^{-1}, defined as the reciprocal of the inter-spike interval, ISI between successive spikes), and firing regularity was quantified by the instantaneous coefficient of variation (CV_2 see Holt et al., 1996; Lee et al., 2019). Poincaré trajectories were constructed by plotting the ISI^{-1} of a spike interval against the ISI^{-1} of the subsequent interval. Averaged ISI^{-1} vs CV_2 plots were constructed as described in Lee et al. (2019).

The neurophysiological properties of each fly were tested in the following sequence with 5 min rest in-between to minimize interference between protocols: flight, LLR and SLR thresholds, LLR refractory period, LLR habituation, SLR refractory period, ability of SLR to follow high frequency stimulation (30 pulses at 200 Hz), and ECS-evoked seizure discharges. Due to the weakness of aged flies and in some cases the absence of LLRs in the last 5% survivors, not all of the flies went through every protocol. If the LLR was absent, all SLR-related protocols were still examined. Generally, all electrophysiological protocols took less than one hour to complete for a single fly.

Statistical Analysis

For each age group tested (1, 5, 50 and 95% mortality), between 7 and 12 flies were generally tested. We have found that this sample size range is often sufficient to draw initial conclusions, based on our previous experiences studying ion channel and 2^{nd} messenger system mutants (Engel & Wu, 1992, 1996; Iyengar & Wu, 2014; Lee & Wu, 2006). Individual flies were considered biological replicates, and all recorded data points were included in the analysis. Due

196 to the non-normal distribution of datasets, the non-parametric Kruskal-Wallis ANOVA test was
197 used to determine cross-sectional differences between physiological parameters of flies from
198 respective genotypes. The rank-sum test (with Bonferroni correction applied) was used as a *post*
199 *hoc* test. Age-dependent trends in physiological parameters were identified by computing the
200 non-parametric Spearman's rank correlation coefficient (r_s) (Sokal & Rohlf, 1969). In the source
201 data files accompanying each figure, the sample mean, median, standard deviation, coefficient of
202 variation and the 25 – 75 %tile interval are listed. To assess the robustness of the respective
203 statistics, a bootstrap resampling approach (Efron, 1981) with 1000 replicates was used to
204 estimate the 95%tile confidence intervals. All statistical analyses were performed in Matlab
205 (r2019b).
206
207 **Results**
208 *Flight Performance and DLM Firing Activity across the Lifespan: Effects of High-Temperature*
209 *Rearing and* Sod *Mutation.*
210 The remarkable flight ability of *Drosophila* has been well documented (Dickinson, 2014;
211 Heisenberg & Wolf, 1984), with flights often lasting for hours in tethered flies (Götz, 1968;
212 Götz, 1987). To assess age-related changes in flight ability over the lifespan, we examined
213 sustained tethered flight (Figure 1A, cf. Iyengar & Wu, 2014) to delineate characterisic
214 alterations in flight muscle electrical activity patterns and corresponding biomechanical
215 parameters, and to reveal the effects of high-temperature and oxidative stressors on the aging
216 process.
217 As established in *Drosophila* and other organisms, the aging process manifests a non-
218 linear progression, indicated by varying rates of mortality at different stages in the lifespan
219 (Figure 1B, cf. Vaupel et al., 1998, see Extended Data Figure 1-1 for the log-transformed
220 mortality rate). We examined WT flies at 25 and 29 ˚C; two commonly used rearing
221 temperatures in *Drosophila* aging studies. As previously reported, at 29 ˚C the fly lifespan was
222 nearly halved as compared to 25 ˚C with a substantially accelerated mortality rate, convenient
223 features frequently used to expedite aging studies (Figure 1B; Leffelaar & Grigliatti, 1983; Loeb
224 & Northrop, 1917; Ruan & Wu, 2008). At both temperatures, however the lifespan trajectories
225 follow an inverse sigmoidal curve, with "plateau", "shoulder" and "tail" phases (Curtsinger et
226 al., 1992). We have also determined the effects of increased oxidative stress by characterizing

Sod mutant flies, reared at a slightly lowered rearing temperature, 23 ˚C rather than 25 ˚C in order to expand the rather short *Sod* lifespan for more precise chronological tracking of data. Notably, in the *Sod* lifespan curve at 23 ˚C, the early plateau phase is absent (Figure 1B), and the slope of the mortality rate is negative across the lifespan (Extended Data Figure 1-1). These distinctive features are previously reported *Sod* life-span curves obtained at higher temperatures (25 or 29 ˚C, Phillips et al., 1989; Ruan & Wu, 2008), and highlight the characteristic high mortality of young *Sod* flies.

We found that flight ability was well-preserved in some aged WT flies reared at either 25 or 29 °C, displaying robust tethered flights beyond the 30-s sustained flight duration, a cut-off criterion which effectively distinguishes flight-defective mutants from WT individuals (Iyengar & Wu, 2014). The "non-fliers" were mostly encountered in flies aged beyond the median lifespan (55 and 30 d for individuals reared at 25 and 29 °C respectively, Figure 1C). In striking contrast, many young *Sod* flies (~50%) were not capable of sustained flight beyond 30 s, and this proportion further increased with age, with few *Sod* flies beyond the median lifespan (9 d) capable of flight beyond 30 s (Figure 1C).

The differences between WT and *Sod* mutants in flight ability prompted us to examine the wing beat frequency (WBF) as well as flight muscle DLM firing rate, across the lifespan. Using protocols established for the tethered flight preparation (Iyengar & Wu, 2014), we were able to acoustically monitor WBF via a microphone and simultaneously record DLM spiking activity (Figure 1A, D). The WBF is largely determined by the natural mechanical resonance frequency of the thorax case, which is powered by alternating activation of two sets of indirect flight muscles, DLMs and dorsal-ventral muscles or DVMs (Chan & Dickinson, 1996). Isometric contraction of indirect flight muscles is stretch-activated and coincides with mechanical oscillation of the thorax, while their spiking activity, occurring at a much lower frequency than WBF, facilitates Ca^{2+} influx for force generation (Dickinson & Tu, 1997; Lehmann & Dickinson, 1997). Therefore, changes in muscle tension without shortening allow microelectrode recordings of the DLM spikes with minimal cell damage during prolonged flight.

Across the lifespan of WT flies, we noted a clear trend of increasing DLM firing rates which nearly doubled in the oldest flies examined (Figure 1D-E, Spearman rank correlation coefficient: $r_s = 0.46$, $p = 9.9 \times 10^{-4}$, and $r_s = 0.58$, $p = 3.6 \times 10^{-4}$, respectively, for 25 and 29 ˚C-reared flies). Accompanying this increasing trend, we noted an apparent overall increase in

variability (Figure 1E, dashed distribution outline). In contrast to this age-associated variability in DLM firing, the WBF showed little change throughout lifespan for the fliers in the three populations. In 25 °C-reared WT flies both young and old individuals displayed average WBF of ~ 190 Hz, with a narrower spread within a +/- 20 Hz (Figure 1F). We observed only a small, but detectable, reduction in frequency across the lifespan of 29 °C reared flies (r_s = -0.41, p = 0.19). Remarkably, the small population of *Sod* fliers displayed largely normal DLM firing rate and WBF with an indicative upward trend in both DLM firing rate and WBF (r_s = 0.50, p = 0.06 and r_s = 0.60, p = 0.018, respectively, Figure 1E-F). Taken together, our analysis of flight patterns suggests that the biomechanical properties of flight remained largely stable across the lifespan, while increases in DLM spiking mean frequency and variability reflected potential age-related alterations in central motor circuits.

In the following sections, we adopt the measure of "biological age", by tracking the percent mortality of the population, in order to facilitate comparisons of the aging trajectories of functional alterations across different genotypes and conditions. This can be achieved by a re-normalization of the time axis to reflect the cumulative mortality based on the chronology lifespan curves (Figure 1B). As shown in the following figures, we collected data at different biological ages, for WT flies reared at 25 ˚C, biological ages at <1%, 5%, 50% and 95% mortality corresponded to the chronological ages of 7, 31, 50 and 72 days, whereas for 29 ˚C rearing, this shifted to 7, 20, 30 and 35 days. Since *Sod* flies lacked a prolonged initial plateau phase but showed a lingering "tail" in the lifespan curve, the biological ages targeted for data collection were modified to compress the first time interval to <5% mortality, and 70% mortality was added before the final 95% stage so as to allow sampling within the prolonged "tail". The stages for *Sod* flies at <5%, 50%, 70%, and 95% mortality therefore corresponded to 2, 9, 14, and 30 days. The distinct profile of *Sod* aging trajectory indicates markedly different effects exerted by oxidative and high temperature stressors on the mortality rate along the lifespan. It is worth noting that despite the early precipitous drop and a shortened population medium lifespan, a small fraction of *Sod* mutant flies nevertheless exhibited relatively prolonged survivorship, giving rise to the characteristic, disproportionally prolonged tail in its lifespan curve.

Age-Resilient and -Vulnerable Properties of the Giant Fiber (GF) Circuit that Mediates a Jump-and-Flight Escape Reflex

One of the best-studied motor circuits in adult *Drosophila* is the giant fiber (GF) pathway that triggers a jump-and-flight escape reflex critical for survival (Figure 2A, cf. Tanouye & Wyman, 1980; Trimarchi & Schneiderman, 1995b; von Reyn et al., 2017). Visual and other sensory inputs to the GF interneuron dendrites in the brain initiate the action potential propagating along the descending axon to drive a set of motor neurons in the thoracic ganglion. The DLM motor neuron receives the GF command signal indirectly via a peripherally synapsing interneuron (PSI) to evoke a DLM spike. This axo-axonal GF-PSI contact has been characterized as a mixed electrical and cholinergic synapse (Allen & Murphey, 2007; Blagburn et al., 1999; Gorczyca & Hall, 1984; King & Wyman, 1980). It has been well established that electric stimuli across the brain evoke two types of GF pathway-mediated DLM responses with distinct latencies (Figure 2B). Low-intensity stimulation across the brain recruits afferent inputs to the GF neuron, thereby triggering a relatively longer latency response (LLR, ~ 4 - 6 ms, Elkins & Ganetzky, 1990; Engel & Wu, 1992, 1996), whereas high-intensity stimuli directly activate GF axonal spikes bypassing the brain afferents and resulting in a shorter latency response (SLR, ~0.8 - 1.6 ms, Engel & Wu, 1992; Tanouye & Wyman, 1980).

We found clear distinctions between SLR and LLR in age-dependent modifications across the lifespan. Figure 2C shows robust maintenance of the basic properties (axonal conduction), of the GF neuron and downstream elements (PSI and DLM motor neurons) in aging WT flies, as indicated by the well preserved SLR parameters (see Table 1 for sample means, standard deviations and coefficients of variation). No significant age-dependent alterations were observed in the latency or threshold of the SLR for either 25 or 29 °C-reared WT flies, consistent with a previous report on well-maintained SLR properties up to a late stage of the lifespan (cf. Martinez et al., 2007). Nevertheless, we did observe a significant change in SLR properties in young *Sod* mutants which displayed a retarded latency compared to 25 °C-reared WT counterparts (SLR latency mean: 1.6 vs 1.1 ms, $p = 0.002$, Kruskal-Wallis ANOVA, Figure 2C, Table 1). Furthermore, we noted an age-dependent decrease in this parameter for *Sod* ($r_s = -0.50$, $p = 0.0015$). This apparently paradoxical improvement brought the SLR latency parameters to a range directly comparable to those of WT flies, likely reflecting a progressive change in the *Sod* population composition, as healthier individuals persist and become better represented, while weaker ones die off.

In contrast to the robust SLR properties, LLR parameters revealed clear changes in afferent inputs from higher centers to the GF neuron. Strikingly, among the oldest WT flies (e.g. 25°C, 95% mortality), LLRs were not elicited in more than half of them (14 of 26), indicating severely compromised afferent inputs to the GF. Additionally, both 25 and 29 °C-reared WT populations displayed a small (< 10%), but detectable, age-dependent increases in LLR latency (r_s = 0.37 and 0.47; p = 0.003 and 0.0005, respectively, see also Table 1), and a modest age-dependent increase in LLR threshold (r_s = 0.57, p = 1.3 x 10^{-5}) was found in 29 °C-reared flies. These relatively stable LLR properties were not grossly disrupted in the *Sod* mutant flies that remained responsive (Figure 2D).

In summary, our SLR results indicate that the GF and its downstream elements, including the PSI and DLM motor neurons remain robust and could reliably transmit vital signals to evoke an escape reflex even in aged flies. However, the input elements upstream to the GF neuron showed more clear age-dependent functional decline, which could lead to a catastrophic collapse of LLR in some of the extremely old individuals (95% mortality) that were devoid of LLR.

Alteration of SLR and LLR Refractory Period by High-Temperature and Oxidative Stressors

The robust, well-maintained basic properties of the GF and its downstream elements provide reliable readouts for examination of activity-dependent plasticity across the lifespan to uncover aging-vulnerable neural elements upstream of the GF neuron. By employing well-established stimulus protocols in the tethered fly preparation for activity-dependent processes, including paired-pulse refractory period, and habituation to repetitive stimulation (Engel & Wu, 1996; Gorczyca & Hall, 1984), we were able to establish modification due to aging in these use-dependent properties, as well as their alterations by high-temperature or oxidative stressors. The refractory period (RP), for both SLR and LLRs, is defined as the shortest interval between paired stimulus pulses at which a second DLM response could be evoked (Figure 3A *inset*). We found WT flies across the lifespan displayed similar SLR RP performance when reared at 25 °C, while 29 °C -reared WT flies displayed an apparent, but not statistically significant trend of increasing RP over the lifespan. In a complimentary set of experiments, we delivered 30 SLR-evoking stimuli at 200 Hz and recorded the number successful responses (FF_{30}). Across the lifespan, both 25 °C and 29 °C-reared flies displayed small alterations in performance, with changes not reaching statistical significance (Extended Data Figure 3-1). The refractoriness of

LLR in older WT flies reared at 25 °C was similar their younger counterparts. However, 29 °C-reared WT flies showed a significant age-dependent increase in LLR RP, most evident in the older populations (Figure 3B, 50 & 95% mortality). Notably, the distributions of SLR and LLR RPs in aged groups showed larger skews with several individuals displaying disproportionally lengthened refractory periods (less pronounced in SLR but most evident in LLR RP, Figure 3B). Furthermore, the oldest groups (95% mortality) consistently displayed the largest coefficients of variation of the LLR refractory periods datasets (Table 1). These observations highlight the stochastic nature of age-related functional deterioration in the upstream circuit elements afferent to the GF pathway.

Remarkably, young *Sod* flies represented the most heterogeneous population among different age groups in terms of refractory periods. Presumably the population included a portion of severely defective, very short-lived individuals that accounted for the initial drop and the diminished plateau phase of the lifespan curve (Figure 1B). Our observations revealed significant lengthening in both SLR and LLR refractory periods in very young (< 5% mortality) *Sod* mutants (SLRs $p < 0.05$, and LLRs, $p < 0.01$, Figure 3A-B, Kruskal Wallis ANOVA, Bonferroni-corrected rank-sum *post hoc* test). Similarly, *Sod* mutants displayed significantly lower FF_{30}. indicating worse performance compared to WT counterparts (Extended Data Figure 3-1). In conjunction with a clear increase in SLR latency (Figure 2C), the RP lengthening point towards severe GF defects in a sub-population of young *Sod* flies. On the other hand, the surviving aged *Sod* mutants showed relatively stable SLR and LLR responses, with less substantial age-dependence beyond 50% mortality (Figure 3A-B).

Aging Progression of Higher-Level Activity-Dependent Signal Processing: Acceleration of LLR Habituation over Lifespan

The above results suggest the functional integrity of the GF and its downstream elements as indicated by SLR performance (Figures 2 & 3) is age-resilient across the lifespan. Nevertheless, high-temperature stress and particularly *Sod* mutation can exert clear effects on activity-dependent aspects of GF-mediated DLM responses, as indicated by refractory period of LLRs (Figure 3B). In *Drosophila*, the jump-and-flight startle reflex shows habituation upon repetitive visual stimulation (Trimarchi & Schneiderman, 1995a), which is recapitulated in the habituation of LLRs (Engel & Wu, 1996). Habituation represents a non-associative form of

learning that involves experience-dependent plasticity in higher functions (Engel & Wu, 2009; Rankin et al., 2009).

To further investigate age-related changes in the plasticity of upstream processing of GF inputs, we examined habituation of LLRs (Engel & Wu, 1996; 1998). Upon evoking LLRs repetitively, the DLM responses habituate, as subsequent stimuli fail to recruit LLRs (Figure 4A). However, LLRs may be rapidly restored following the application of a dis-habituation stimulus of a different modality, such as an air-puff, excluding sensory adaptation or motor fatigue as the basis for LLR failure (Figure 4A). We applied 100 LLR-evoking stimuli at three frequencies (1, 2 and 5 Hz), and adopted a habituation criterion as the number of stimuli required to reach 5 consecutive LLR failures (F5F, Figure 4A-B, cf. Engel & Wu 1996). The large number of stimuli used in this protocol provides greater power to resolve age-dependent alterations in an intrinsically stochastic process.

Across the three stimulation frequencies examined (1, 2 and 5 Hz) for WT flies reared at 25 °C, we found that between < 1% and 5% mortality, during the plateau portion of the lifespan, the LLR habituation rate was largely unaltered with a large fraction of flies showing little habituation throughout the stimulation train (Figure 4C-E). However, during the mortality phase of the lifespan curve, 50% mortality and beyond, we observed a marked acceleration in LLR habituation, with the oldest flies habituating the fastest (r_s between -0.33 to -0.56, $p < 0.001$). As expected, we found more evident acceleration in habituation rate at higher stimulation frequencies (Figure 4C-E), which was most pronounced in the older populations (50 & 95 % mortality) examined. Together, our findings suggest that the brain circuits afferent to the GF pathway remained largely unaltered during the plateau portion of the lifespan curve, a substantial fraction of the lifespan. Nevertheless, across the lifespan, we could delineate the distinct habituation rates associated with the 5%, 50% and 95% age groups, particularly at the higher simulation frequency of 5 Hz, offering a quantifiable index of aging progression.

High temperature rearing and *Sod* mutations further accelerated habituation. Compared to 25 ˚C-reared counterparts, 29 ˚C-reared WT flies displayed considerably faster habituation to 1 Hz stimulation in aged groups (50 and 95 % mortality, Figure 4E vs. F). Furthermore, *Sod* mutants (at 23 ˚C) showed an accelerated habituation rates compared to WT counterparts even in younger flies (< 5% mortality, Figure 4G vs, E & F), presumably correlated with the pronounced increase in LLR paired pulse refractory period in this age group (Figure 3B). Therefore, among

412 the temperature- or oxidation-stressed groups, the habituation rate again can serve as a
413 physiological marker of age progression even at low frequencies (~1 Hz) of repetitive
414 stimulation.
415
416 *Increasing Susceptibility to Electroconvulsive Induction of Seizures across the Lifespan*
417 In addition to acting as an output of the flight pattern generator and GF pathway-
418 mediated escape reflex described above, DLM action potentials may serve as reliable indicators
419 of CNS spike discharges associated with seizures (Lee & Wu, 2002; Pavlidis & Tanouye, 1995).
420 Such seizure episodes may reflect aberrant spiking originating from motor pattern generators
421 located in the thorax, such as flight (Harcombe & Wyman, 1977; Iyengar & Wu, 2014) and
422 grooming (Engel & Wu, 1992; Lee et al., 2019). As shown in Figure 5A, high-frequency
423 stimulation across the brain (200-Hz, 2-s train of 0.1-ms pulses, Lee & Wu, 2002) can trigger a
424 highly stereotypic electroconvulsive seizure (ECS) discharge repertoire, consisting of an initial
425 discharge (ID), a period of paralysis reflected by GF pathway failure (F, in response to 1-Hz test
426 pulses), and a second delayed discharge (DD) of spikes. This experimental protocol provides
427 several stable and quantitative measures, within individual flies, suitable for assessing age-
428 related modifications of CNS function, including the threshold to induce seizures (by adjusting
429 intensity from 15 to 80 V, Figure 5B) and the discharge duration of DD spike trains (Figure 5C).
430 We found a clear trend of increasing seizure susceptibility with age in WT and *Sod* flies (Figure
431 5B). WT flies reared either at 25 or 29 ˚C displayed a substantial reduction in the DD threshold
432 across their lifespan (-33% and -23% respectively for <1% vs. 95% mortality). In *Sod* mutants,
433 the trend was even more pronounced (-46 % for 5 % vs. 95 % mortality). The effects of the *Sod*
434 mutation were most striking in the youngest age group. In these flies (< 5% mortality), threshold
435 was significantly higher than WT counterparts ($p < 0.001$, Kruskal-Wallis ANOVA, rank-sum
436 *post hoc*), corroborating the other observations of extreme physiological defects found in this age
437 group (Figures 2 & 3). Furthermore, this increase in ECS threshold was present across the *Sod*
438 lifespan ($p < 0.05$, Kruskal-Wallis ANOVA, rank-sum *post hoc*) suggesting that elevated
439 oxidative stress could render seizure-prone circuits less excitable.
440 Despite individual variability within each fly group, significant correlation coefficients
441 suggest an enhanced excitability of seizure-prone circuits in aged flies (Figure 5B). Compared
442 with other potential indicators, e.g. habituation rate (Figure 4), this age-dependent monotonic

443 decrease of ECS threshold could provide as a tighter, more quantitative measure of aging
444 progression.

445 In contrast to the decreasing trend of seizure threshold over lifespan, there was a milder
446 trend of increasing DD duration in WT flies reared at 29 ˚C, or in *Sod* mutants, but ending with a
447 substantial drop in the oldest (95%) populations (Figure 5C, $r_s = 0.36$, $p = 0.0041$; and 0.34, $p =$
448 0.047 for WT 29 ˚C and *Sod* respectively). However, there was no clear age-dependent trend of
449 increasing DD duration in 25 ˚C-reared WT flies (Figure 5C). In a complementary data set
450 acquired at higher temporal resolution to resolve individual spikes, we examined the total
451 number of spikes during the DD in these populations. Mirroring the DD duration observations,
452 we found that 25 ˚C-reared WT flies did not display an age-dependent trend, while WT flies
453 reared at 29 °C, as well as *Sod* mutants, showed modest increases in the DD spike count
454 (Extended Figure 5-1, $r_s = 0.50$, $p = 1.4 \times 10^{-5}$ for WT 29 ˚C; $r_s = 0.27$, $p = 0.04$ for *Sod* mutants).
455
456 *Age-Trajectories of ID Firing Patterns Reveal a Potential Predictor of Mortality Rate*

457 Alterations in ECS threshold and DD duration across life span (Figure 5) call for detailed
458 characterization of ID spiking to extract additional salient features associated with aging
459 progression. Since ID occurs as a brief burst (1 – 4 s, see Figures 5A and 6A) of high-frequency
460 spiking activity, a set of ECS data at a higher temporal resolution enabled an analysis of ID
461 spiking dynamics at the level of individual spikes (Figure 6A). Immediately following
462 electroconvulsive stimulation, the ID spike patterns manifested striking, but more complex, age
463 dependence and vulnerability to oxidative stress. In younger WT flies (reared at either 25 or 29
464 ˚C), ID spike counts progressively increased with age until about 50% mortality (Figure 6A and
465 B). Beyond 50% mortality, a decline in the ID spike count became apparent; notably the oldest
466 flies (95% mortality) regressed to a spike count similar to those of young flies (< 1% mortality).
467 In contrast to nearly 10-fold range for ID spike counts across the WT lifespan, *Sod* mutants
468 displayed only rather sparse spiking, too few to shape a prominent age-related profile in their
469 counts (Figure 6A and B). This observation mirrors the particular vulnerability of ECS
470 discharges to oxidative stress, along with the drastically elevated threshold levels in ECS
471 induction in *Sod* mutant flies (Figure 5B).

472 We noted that the curve of average ID spike count across the lifespan showed a gross
473 resemblance in overall profile with the mortality rate curve. The progression of spike count

474 changes apparently preceded the mortality rate changes in WT (compare Figure 6B and C). We
475 sought an appropriate temporal shift between the ID spike count and mortality rate curves that
476 would optimize regression fit. The iterations yielded the best correlation between the ID spike
477 count and mortality rate with 11- and 6-d lags for WT flies reared at 25 and 29 ˚C, respectively
478 (Figure 6D and E). These observations suggest that the ID spike production over the lifespan
479 may serve a predictor for the ensuing mortality rate in WT flies. In other words, along with other
480 physiological indicators for aging progression examined above (Figures 4 and 5B), ID spike
481 counts might also provide a gross forecast of the mortality rate, which is the derivative of the
482 lifespan curve. However, this relationship may not be applicable to a variety of genotypes since
483 it does not seem to hold true for *Sod* flies (Figure 6A and B).
484
485 *Signatures of ID Spiking Patterns in Young and Old WT and Sod Flies*
486 Salient features of spike patterns can be uncovered by systematical tracking of the
487 successive changes in consecutive spike intervals to depict the spike train dynamics, as shown in
488 the Poincaré plots (Figure 6F, cf. Lee et al., 2019). In these plots, instantaneous firing frequency,
489 defined as the inverse of an inter-spike interval (ISI^{-1}), was first determined for each of the
490 successive spike intervals in a spike train. Each ISI^{-1} was then plotted against the ISI^{-1} of the
491 following spike interval and the process was reiterated sequentially for each spike in the ID spike
492 train (i.e. ISI^{-1}_{i} vs. ISI^{-1}_{i+1} for the i^{th} spike in the sequence). For strictly periodic spiking, all data
493 points of the Poincaré trajectory (PT) would fall at a single location along the diagonal. Irregular
494 deviations from rhythmicity between successive spike intervals appear as perpendicular shifts
495 away from the diagonal. Thus, the trajectory depicts the evolution of spiking frequency, while
496 excursion patterns about the diagonal in the PT indicate characteristics of recurrent firing
497 patterns. Poincaré plots of representative individual spike trains are shown in Figure 6F that
498 readily capture the larger number of spikes with increasing ISI^{-1} in aged WT flies compared to
499 younger counterparts (up to 100 Hz vs. < 30 Hz). In contrast, the few ID spikes in *Sod* flies,
500 regardless of age, occurred in a lower frequency range (~10 Hz).
501 To integrate information embedded in individual PTs to indicate overall differences in ID
502 spiking dynamics between age groups, we replotted the PTs to carry both frequency and local
503 variation for successive ISIs in order to combine them into an 'average' trajectory (Figure 6G,
504 see Methods and Lee et al., 2019 for computational details). Briefly, for each ISI in the ID spike

sequence, the ISI^{-1} was plotted against the instantaneous coefficient of variation (CV_2), defined as: $2 | ISI^{-1}_i - ISI^{-1}_{i+1}| / [ISI^{-1}_i + ISI^{-1}_{i+1}]$ (Holt et al., 1996). Along the trajectory, low CV_2 values correspond to more regular firing (lower fractional changes among adjacent spike intervals), while high CV_2 values indicate where more abrupt changes in spike intervals occur. The IDs of young WT flies (< 1% mortality) reared at either 25 ℃ or 29 ℃ displayed rather similar ISI^{-1} vs CV_2 trajectories compared to each other, with peak ISI^{-1} between 10 and 20 Hz and a similar range of CV_2 in the spiking procession. Remarkably, for both rearing temperatures, the trajectories of aged WT flies displayed similar transformation from their young counterparts, with more complex, right-shifted trajectories with peak ISI^{-1}s > 70 Hz (Figure 6G, 41 – 50 d and 21-30 d, respectively, for 25 ℃ and 29 ℃-rearing), suggesting that the changes in circuit activity patterns across lifespan are conserved during high-temperature rearing. Nevertheless, the simple ISI^{-1} vs CV_2 trajectories of both young and aged *Sod* stood in sharp contrast to WT trajectories, providing another major distinction between the effects of high-temperature and oxidative stressors and underscoring the hypoexcitable nature of the *Sod* mutant.

Clearly, these "average" trajectories present concisely the overall characteristics of the ID spiking activity, with precise temporal information from the initiation to cessation of the spike train. They are effective signatures for IDs of different age groups in each genotype; WT flies reared at 25 and 29 ℃ traverse similar terrains in the span of ID spike trains whereas *Sod* flies of various ages yield only abbreviated signatures, marking very limited terrains in specific regions in the frequency-variance landscape.

Discussion

This report summarizes our initial efforts towards a quantitative description of neurophysiological changes during aging in several well-established motor circuits in *Drosophila*. Aging studies in flies have largely focused on how the lifespan is influenced by genetic modifications in cellular biochemical pathways, such as those regulated by insulin-like peptide (e.g. Clancy et al., 2001; Hwangbo et al., 2004) and target of rapamycin (e.g. Kapahi et al., 2004) signaling and oxidative stress (e.g. Phillips et al., 2000; Tower, 1996), as well as by environmental factors, including diet (e.g. Mair et al., 2003; Piper & Partridge, 2007; Skorupa et al., 2008) mating experience (Gendron et al., 2014; Harvanek et al., 2017; Kuo et al., 2012), exercise (Piazza et al., 2009; Sujkowski et al., 2015), and trauma (Katzenberger et al., 2015;

Katzenberger et al., 2013). In parallel, several established behavioral assays have provided readouts of age-related functional decline, including: fast phototaxis and negative-geotaxis (e.g. Arking & Wells, 1990; Miquel et al., 1976; Simon et al., 2006), flight (Miller et al., 2008), memory (Tamura et al., 2003; Yamazaki et al., 2007), courtship (Cook & Cook, 1975; Partridge et al., 1987), as well as sleep and other circadian activity patterns (Bushey et al., 2010; Koh et al., 2006). However, behavior-relevant studies registering concomitant changes in neurophysiological processes in *Drosophila* have been largely limited to electroretinogram (Ueda et al., 2018), peripheral neuromuscular synapses (Banerjee et al., 2021), or GF pathway SLR properties (Augustin et al., 2018; Augustin et al., 2019; Blagburn, 2020; Martinez et al., 2007). Our work provides an initial glimpse across an array of motor circuits including the upstream processing of the GF-mediated escape circuit, and pattern generators driving flight and seizure discharges. Furthermore, our observations provide a first-order quantitative comparison of age-trajectories, revealing drastically different effects of high-temperature rearing and oxidative stress on the aging-progression of various neurophysiological parameters in WT and mutant flies.

Aging-Resilient and -Vulnerable Aspects of Motor Circuit Function in Drosophila

In this study, we adopted a normalization in time scales of aging progression in accordance with % mortality (Jones et al., 2014) to facilitate comparisons across the genotypes and conditions that yield drastically different chronological lifespan curves (Figure 1B). A graphical overview emerges when comparing the age-trajectories of the various motor circuit parameters in different fly populations. Relative to the starting point (i.e. youngest age group), changes (in fold on a semi-logarithmic $\log_2$ scale) in various circuit functions can be compared directly for their relative vulnerability or resilience to aging (Figure 7).

Our results suggest the operation and integrity of motor circuits fall into two general categories: aging-resilient (Figure 7, lighter shading) and -vulnerable (darker shading). Notably, the elements in the GF pathway that mediate the escape reflex appear more robust and show less functional decline up to the very end of the lifespan and display milder effects of high-temperature stress or ROS scavenger disruption, with little impact on SLR and LLR threshold and latency (Figure 7B-1, -2, -4 and -5). In contrast, substantial changes were seen in the more plastic, use-dependent, functions of these circuit components, including the twin-pulse refractory

period of the GF pathway and the habituation of its afferent inputs (Figure 7B-3, -6, and -9). Furthermore, motor program-related DLM spike readouts, such as the flight and ECS discharge patterns, showed remarkable age-related modifications (Fig 7B-8, -10, -11 and -12).

GF Pathway SLRs: GF Neuron and Downstream Elements

The GF pathway with its well-described neural elements and transmission properties offers an ideal model system to explore cellular mechanisms of aging and neurodegenerative diseases, as previously reported for its SLR properties (Augustin et al., 2018; Martinez et al., 2007; Sofola et al., 2010; Zhao et al., 2010). Consistently, our characterization of SLRs underlying the escape reflex demonstrates robustly maintained basic mechanisms, for signal propagation from the GF neuron through the PSI and DLM motor neuron to postsynaptic DLMs. Over a large portion of the lifespan, including the oldest flies (95% mortality), WT flies reared at both room 25 and 29 °C-did not show a clear trend of increase or decrease in either SLR latency or threshold, but a decreasing trend in both threshold and latency was noted in *Sod* mutant flies, indicating a consequence of chronic oxidative stress (Figure 2C, Figure 7B-1 and -2).

More evident aging-vulnerable alterations were seen in the activity-dependent properties for flies grown under high-temperature or ROS stressors. For WT reared at 25 °C, frequency-dependent characteristics of the SLR, including the twin-pulse RP and FF_{30}, were relatively stable with no statistically significant age-dependent changes detected (Figure 3A and Table 1). However, this is not the case for 29 °C-reared WT or *Sod* mutant flies since detectable but opposite trends of changes were observed in these two categories of flies in both twin-pulse RP and FF_{30} readouts (Figure 3A, Figure 7B-3, Table 1), suggesting differential effects on certain vulnerable properties by these two types of stressors (e.g. mechanisms underlying axonal conduction and/or synaptic transmission).

GF Afferent Processing: LLR Refractory Period and Habituation

The processing of afferent signals from upstream circuits activates the GF LLRs (Figure 7A). Similar to SLRs, we found activity-dependent properties of LLRs, i.e. RP and habituation were more markedly modified over the lifespan than the subtle changes in latencies and thresholds (Figures 2D, 3B, 4; Table 1; Figure 7B-4 and -5). Given the apparent stability of transmission of the GF neuron and downstream elements, these changes hint at age-dependent

plasticity in GF afferents in the brain (Engel & Wu, 1996; 1998), presumably in identified visual (Ache et al., 2019) or mechanosensory (Blagburn, 2020; Lehnert et al., 2013; Mu et al., 2014) inputs.

We observed increasing trends of LLR latency and threshold as flies age (Figures 2D; Table 1; Figure 7B-4 and -5). However, even though age-dependent alterations observed in LLR latency are statistically significant, they are relatively minor in magnitude, constituting only small fractions in time scale within a 5-20 ms behavioral repertoire for visually or olfactorily triggered GF-mediated escape responses (Engel & Wu, 1992, 1996; Trimarchi & Schneiderman, 1995a; von Reyn et al., 2017).

We also noted that the LLR RP determined by the paired-pulse protocol revealed substantial heterogeneity in the older WT populations examined as indicated by extremely large spread of data points (50 and 95% mortality at 25 and 29 °C, Figure 3B, Table 1), indicating the stochastic nature of aging progression in GF afferent signal processing.

Importantly, the LLR habituation protocol (Engel & Wu, 1996; 1998) demonstrated clearest monotonic age-dependent changes in the performance of the GF pathway. In both 25 and 29 °C-reared WT, as well as *Sod*, populations, aged flies habituated much faster compared to younger counterparts (Figure 4, Figure 7B-9). Consistent across all populations, these effects were evident for all frequencies tested (1, 2, and 5 Hz, with r_s coefficients ranging from 0.33 to 0.56 and with significant *p* values). Furthermore, habituation is commonly considered a simple form of non-associative learning (Engel & Wu, 2009; Rankin et al., 2009). Our observation that the *Drosophila* GF habituation rate increases monotonically and robustly with age (Figures 4 and 7B-9) renders this plasticity parameter a potential quantitative index of aging progression for an important aspect of nervous system function.

Flight

Throughout most of their lifespan, WT flies maintained their flight ability (Figure 1C) with stable WBFs (Figure 1D, F; Figure 7B-7), suggesting the presence of effective homeostatic adjustments to overcome aging-associated changes in biomechanical properties of flight muscles and thoracic case. As previously reported (Miller et al., 2008), WBF is stable beyond the median lifespan in spite of marked changes in muscle structure and stiffness (see also Chaturvedi et al., 2019). Despite the nearly invariant WBFs, we found the flight pattern generator circuit driving

DLM displayed a clear and largely monotonic increase in firing rate with age (Figure 1E, Figure 7B-8), a robust phenotypic change in both 25 ˚C and 29 ˚C-reared flies. Conceivably, the age-dependent increases in firing rate could indicate changes in motoneuron (DLMn) excitability or flight patterning circuit signal processing among the relevant thoracic interneurons. In either case, this provides a compensatory mechanism to ensure flight ability as aging progresses, namely, increasing the firing rate of muscle Ca^{2+} action potential to retain appropriate intracellular Ca^{2+} levels for powering sustained flight in myogenic stretch-activated DLMs (Gordon & Dickinson, 2006; Lehmann et al., 2013; Pringle, 1978).

Electroconvulsive Seizure

In tethered flies, high frequency stimulation across the brain recruits a remarkably stereotypic pattern of nervous system-wide spike discharges accompanied by wing-buzzes (in a fixed succession of ID, paralysis, and DD, cf. Lee & Wu, 2002), reminiscent of the sequence of seizures and paralysis induced by mechanical shock in “bang-sensitive” mutants (Burg & Wu, 2012; Ganetzky & Wu, 1982). Importantly, the spiking associated with the ID and DD is independent of the GF system; during the ECS repertoire, transmission along the escape pathway is blocked (Pavlidis & Tanouye, 1995). Analysis of decapitated flies and Ring-X gynandromorph mosaics has further indicated that both ID and DD pattern generators reside in the thorax, although globally synchronized electric activities and quiescence episodes concurrent with the ID-paralysis-DD repertoire also emerge along the body axis (Lee & Wu, 2002) and across the brain (Iyengar & Wu, 2021). However, the ID and DD are likely derived from separable network origins, as they are independently vulnerable to different ion channel mutations (Kasuya et al., 2019; Lee & Wu, 2006).

In both WT and *Sod* flies, we noted a clear age-dependent decrease in the threshold of ECS-evoked seizure across the lifespan (Figure 5, Figure 7B-10). The monotonic characteristic of this reduction suggests seizure threshold may be considered as another quantitative index of the age progression in nervous system function. Indeed, aged rats reportedly show reduced threshold for kainate-induced seizures (Liang et al., 2007) and elderly humans display increased incidence of seizure disorders (Leppik et al., 2006; Tallis et al., 1991).

ECS discharge spiking patterns exhibit age-dependent trajectories as well (Figure 7B-11 and -12), most dramatically during the ID phase (Figure 6). Instead of a monotonic trend, ID

spiking increases initially with age, peaking around 50% mortality, then declines to earlier levels towards the end of the lifespan (Figures 6B and 7B-11). It is also intriguing to see that changing ID spiking intensity seemingly provides a forecast for subsequent mortality rate. Indeed, with appropriate lags (11 d. and 6 d. For 25 and 29 °C-reared flies), there are high degrees of cross-correlation between the two parameters (Figure 6F & G). It would be interesting to examine this relationship in additional mutants with intrinsically altered neuronal excitability and lifespan. For example, both hyper-excitable *Shaker* (*Sh)* and hypo-excitable mle^{napts} (nap^{ts}) mutants display shortened lifespans (Reenan & Rogina, 2008; Trout & Kaplan, 1970) along with drastically altered ECS discharges (Lee & Wu, 2006), flight pattern generation (Iyengar & Wu, 2014, unpublished observations), and habituation (Engel & Wu, 1998).

Distinctive Patterns of Aging-Related Changes by High Temperature and Oxidative Stress

The distinct aging trajectories manifested in the functioning of the various motor circuits described above clearly delineate the manners in which high-temperature rearing and oxidative stress, imposed by external environment versus internal milieu, differ in their effects on aging progression in motor functions.

Ambient temperature is a key factor in determining lifespan in *Drosophila* (Loeb & Northrop, 1917) and other ectotherms. Rearing at high temperature (29 °C), lifespan is shortened by ~ 40-50 % compared to 25 °C, (Figure 1B). Our data support the notion that aging progression is faster at 29 °C but it largely retains the characteristics of the motor performance trajectories of 25 °C, as though it proceeds at a "compressed" time scale. Parameters that were age-resilient in 25 °C-reared flies were robustly maintained in 29 °C-reared individuals (SLR and LLR latency and threshold, flight WBF, Figure 7B *lighter shade*). Similarly, age-vulnerable parameters generally preserved consistent trends in age-dependent changes when scaled for % mortality. This is true particularly for increased DLM firing frequency during flight, increased LLR habituation rate, and decreased ECS seizure threshold (Figure 7B-8, -9, -10 *darker shade*). Remarkably, even the bell-shaped age profile of ID spiking was retained in the 29 °C-reared WT population (Figure 7B-11). For the remaining parameters, SLR and LLR refractory periods, habituation and DD spiking, 29 °C-rearing appeared to intensify their age-dependence, leading to considerably steeper trends (Figure 7B-3, -6, -12). Our findings suggest that in the shortened lifespans of temperature-stressed individuals, the temporal characteristics of neurophysiological

changes is largely retained, albeit "accelerated" according to the degree of lifespan compression. Importantly, these observations give justification for the common practice of using 29 °C-rearing to expedite experiments in *Drosophila* aging studies.

Our findings from *Sod* mutants indicate that oxidative stress exerts strong influences on some physiological parameters with outcomes distinct from the effects of high-temperature rearing. Oxidative stress, resulting from inefficient clearance of metabolic reactive oxygen species (ROS, e.g. superoxide anion and other free radical species), is thought as a major contributor to aging processes (Finkel & Holbrook, 2000; Harman, 1956; Harman, 1981). A key class of ROS scavenging enzymes is the Superoxide dismutases which convert superoxide anions into hydrogen peroxide (Hart et al., 1999; Miller, 2012). In *Drosophila*, three Superoxide dismutase (Sod) enzymes have been identified: intracellular Cu^{2+}/Zn^{2+} Sod1 (encoded by *Sod*, Phillips et al., 1989), mitochondrial Mn^{2+} Sod2 (encoded by *Sod2*, Duttaroy et al., 2003; also known as *bewildered*, Celotto et al., 2012), or extracellular Sod3 (encoded by *Sod3*, Jung et al., 2011). Stress resistance and longevity of the fly are greatly compromised when any of the three is disrupted. Indeed, the *Sod* allele described in this study has no detectable enzymatic activity (Phillips et al., 1989), and exhibits locomotor defects as well as sensitivity to mechanical-, paraquat- and heat-stress along with greatly shortened lifespan (Ruan & Wu, 2008).

Across the *Sod* populations, the general trend still holds true in that the identified age-resilient parameters could sustain functionality throughout the lifespan (GF SLR and LLR latency and threshold, flight WBF, Figure 7B *lighter shade*). For several aging-vulnerable properties, *Sod* flies also follow the general profile of age progression albeit with modified amplitude of expression. These are apparent in DLM firing during flight and ID spiking (Figure 7B-8, -11), and more notably, in both accelerated rate of habituation and reduced ECS seizure threshold, closely resembling the corresponding age-trajectories in WT counterparts (Figure 7B-9 and -10). Nevertheless, more striking alterations in *Sod* are seen in the activity-dependent properties of the GF pathway, as reflected in the trajectories of refractory period for both SLR and LLR that are clearly distinct from high-temperature effects (Figure 7B-3, -6).

A unique feature of the aging trajectories of *Sod* motor functions is the apparent anomaly in some age groups that exhibit unexpected trends in phenotypic extremity. Among different age groups of *Sod* mutants, the youngest age group (< 5% mortality) displayed the most conspicuous deviations from the WT counterpart in several categories of motor performance (Figure 7B),

including diminished flight ability (Figure 1C), longer SLR latency (Figure 2C), lengthened SLR and LLR refractory periods (RP, Figure 3), increased ECS threshold (Figure 5B), and decreased spiking during seizure discharges (Figures 5C & 6B). These parameters were often accompanied by a greater spread in measurements among the youngest *Sod* flies (e.g. Figures 3A & B; 5B). Intriguingly, the aged *Sod* flies (70 & 95% mortality) paradoxically performed at levels comparable to their aged WT counterparts (Figure 7B), as though they could outperform the young mutant flies. ~~These findings are shared by an independently isolated loss-of-function *Sod* allele (*Sod*^{21}, Ueda, Iyengar & Wu, 2021).~~ It is possible that secondary mutations in the *red* genetic background contribute to the observed differences between the *Sod* mutants and their WT counterparts, as genetic background effects can have profound effects on specific aging phenotypes (Partridge & Gems, 2007). However, observations from an independently generated loss-of-function *Sod* allele (*Sod*^{21}) revealed a similar set of GF transmission phenotypes in young *Sod*^{21} flies (<5% mortality), including a retarded SLR response latency and a poor ability for SLRs to follow high-frequency stimulation (Ueda et al., 2021). Thus, unidentified modifiers in the background are an unlikely explanation for the respective *Sod* phenotypes reported here, which can be seen even in the youngest adult *Sod* populations.

A likely explanation for this seemingly counterintuitive trend could be the highly stochastic nature of oxidative insults in both development and function of neural circuits such that a portion *Sod* flies carry more severe but variable in-born defects, compounding the manifestation of aging progression. distinct from aging processes. Therefore, the *Sod* mutant population undergoes a progressive selection over time in favor of healthier individuals while those with poor circuit performance die off earlier. Consistent with this view, *Sod* mutants reportedly have difficulty eclosing from their pupal case (Phillips et al., 1989; Şahin et al., 2017; Woods, 2017) and the *Sod* lifespan curve lacks the earlier plateau phase (Figure 1B) resulting from much higher mortality in young individuals compared to WT populations. This possibility is further highlighted in a recent study demonstrating certain differences in functional consequences of oxidative stress imposed chronically throughout development in mutant flies and those resulting from acute induction by drug feeding to healthy flies. In WT flies, elevated ROS levels induced by paraquat feeding lead to a distinct collection GF transmission phenotypes compared to *Sod* mutants (Ueda et al., 2021). For example, the SLR latency and refractory period defects in *Sod* mutants are not observed in paraquat-fed WT flies.

Physiological Hallmarks of Aging Progression in Motor Circuits: Quantitative Biomarkers

It is desirable to search for potential physiological aging indices to completement existing cellular and molecular biomarkers of aging in *Drosophila*, such as erroneous expression of the transcription factor genes *wingless* and *engrailed* (Rogina et al., 1997), accumulation of glycation end-products (Baynes, 2001; Jacobson et al., 2010; Oudes et al., 1998) and heat-shock protein (Landis et al., 2004; Tower, 2011), as well as modified functional states of the insulin and TOR signaling pathways components (Kapahi et al., 2004; Partridge et al., 2011).

Among the various age-dependent trajectories in motor circuit performance, two protocols, LLR habituation and ECS induction, yielded parameters that displayed remarkably consistent aging progressions in normal, high temperature-reared and ROS-stressed populations. Specifically, both acceleration of the habituation rate (Figures 4) and reduction in ECS seizure threshold (Figures 5B) displayed a relatively uniform, monotonic age-trajectories (Figure 7B-9 and -10), providing an unambiguous read-out of the circuit performance index along the percent mortality axis. It will be particularly interesting to examine whether the age-trajectories of these parameters are similarly scaled against lifespan in long-lived flies such as WT flies under calorie restriction conditions or in *chico* and other insulin pathway mutants. Furthermore, future studies can utilize these physiological properties to study the relationships between life-span and health-span in the context of various environmental conditions, pharmacological interventions or genetic manipulations which affect longevity.

~~Future studies will further evaluate their suitability as readily accessible, quantitative indices for more incisive aging assessment in WT and mutant flies. This will be a desirable addition in aging research using a wealth of available mutants, such as insulin signaling pathway mutants that are known to affect lifespan, under various environmental conditions, pharmacological manipulations or influences of interacting genes.~~

References

Allen, M. J., & Murphey, R. (2007). The chemical component of the mixed GF-TTMn synapse in Drosophila melanogaster uses acetylcholine as its neurotransmitter. *European Journal of Neuroscience, 26*(2), 439-445.

Arking, R., & Wells, R. A. (1990). Genetic alteration of normal aging processes is responsible for extended longevity in Drosophila. *Developmental Genetics, 11*(2), 141-148. doi:10.1002/dvg.1020110204

Atwood, H. (1992). Age-dependent alterations of synaptic performance and plasticity in crustacean motor systems. *Experimental Gerontology, 27*(1), 51-61.

Augustin, H., McGourty, K., Allen, M. J., Adcott, J., Wong, C. T., Boucrot, E., & Partridge, L. (2018). Impact of insulin signaling and proteasomal activity on physiological output of a neuronal circuit in aging Drosophila melanogaster. *Neurobiology of Aging, 66*, 149-157. doi:10.1016/j.neurobiolaging.2018.02.027

Augustin, H., Zylbertal, A., & Partridge, L. (2019). A Computational Model of the Escape Response Latency in the Giant Fiber System of Drosophila melanogaster. *Eneuro, 6*(2). doi:10.1523/eneuro.0423-18.2019

Banerjee, S., Vernon, S., Jiao, W., Choi, B. J., Ruchti, E., Asadzadeh, J., . . . McCabe, B. D. (2021). Miniature neurotransmission is required to maintain Drosophila synaptic structures during ageing. *Nature Communications, 12*(1), 4399. doi:10.1038/s41467-021-24490-1

Baynes, J. W. (2001). The role of AGEs in aging: causation or correlation. *Experimental Gerontology, 36*(9), 1527-1537. doi:10.1016/s0531-5565(01)00138-3

Biteau, B., Karpac, J., Supoyo, S., DeGennaro, M., Lehmann, R., & Jasper, H. (2010). Lifespan extension by preserving proliferative homeostasis in Drosophila. *Plos Genetics, 6*(10), e1001159.

Blagburn, J. M. (2020). A new method of recording from the giant fiber of Drosophila melanogaster shows that the strength of its auditory inputs remains constant with age. *PloS One, 15*(1), e0224057. doi:10.1371/journal.pone.0224057

Blagburn, J. M., Alexopoulos, H., Davies, J. A., & Bacon, J. P. (1999). Null mutation in shaking-B eliminates electrical, but not chemical, synapses in the Drosophila giant fiber system: a structural study. *Journal of Comparative Neurology, 404*(4), 449-458.

Burg, M. G., & Wu, C. F. (2012). Mechanical and temperature stressor-induced seizure-and-paralysis behaviors in Drosophila bang-sensitive mutants. *Journal of Neurogenetics, 26*(2), 189-197. doi:10.3109/01677063.2012.690011

Bushey, D., Hughes, K. A., Tononi, G., & Cirelli, C. (2010). Sleep, aging, and lifespan in Drosophila. *BMC Neuroscience, 11*, 56. doi:10.1186/1471-2202-11-56

Campbell, S. D., Hilliker, A. J., & Phillips, J. P. (1986). Cytogenetic analysis of the cSOD microregion in Drosophila melanogaster. *Genetics, 112*(2), 205-215.

Celotto, A. M., Liu, Z., Vandemark, A. P., & Palladino, M. J. (2012). A novel Drosophila SOD2 mutant demonstrates a role for mitochondrial ROS in neurodevelopment and disease. *Brain Behav, 2*(4), 424-434. doi:10.1002/brb3.73

Chan, W. P., & Dickinson, M. H. (1996). In vivo length oscillations of indirect flight muscles in the fruit fly Drosophila virilis. *Journal of Experimental Biology, 199*(Pt 12), 2767-2774.

824 Chaturvedi, D., Prabhakar, S., Aggarwal, A., Atreya, K. B., & VijayRaghavan, K. (2019). Adult
825 Drosophila muscle morphometry through microCT reveals dynamics during ageing.
826 *Open Biol*, *9*(6), 190087. doi:10.1098/rsob.190087
827 Clancy, D. J., Gems, D., Harshman, L. G., Oldham, S., Stocker, H., Hafen, E., . . . Partridge, L.
828 (2001). Extension of life-span by loss of CHICO, a Drosophila insulin receptor substrate
829 protein. *Science*, *292*(5514), 104-106. doi:10.1126/science.1057991
830 Cook, R., & Cook, A. (1975). The attractiveness to males of female Drosophila melanogaster:
831 effects of mating, age and diet. *Animal Behaviour*, *23*(3), 521-526. doi:10.1016/0003-
832 3472(75)90129-3
833 Curtsinger, J. W., Fukui, H. H., Khazaeli, A. A., Kirscher, A., Pletcher, S. D., Promislow, D. E.,
834 & Tatar, M. (1995). Genetic variation and aging. *Annual Review of Genetics*, *29*(1), 553-
835 575.
836 Curtsinger, J. W., Fukui, H. H., Townsend, D. R., & Vaupel, J. W. (1992). Demography of
837 genotypes: failure of the limited life-span paradigm in Drosophila melanogaster. *Science*,
838 *258*(5081), 461-463. doi:10.1126/science.1411541
839 Dickinson, M. H. (2014). Death Valley, Drosophila, and the Devonian toolkit. *Annual Review of*
840 *Entomology*, *59*, 51-72. doi:10.1146/annurev-ento-011613-162041
841 Dickinson, M. H., & Tu, M. S. (1997). The function of dipteran flight muscle. *Comparative*
842 *Biochemistry and Physiology Part A: Physiology*, *116*(3), 223-238.
843 Duttaroy, A., Paul, A., Kundu, M., & Belton, A. (2003). A Sod2 null mutation confers severely
844 reduced adult life span in Drosophila. *Genetics*, *165*(4), 2295-2299.
845 Efron, B. (1981). Nonparametric estimates of standard error: the jackknife, the bootstrap and
846 other methods. *Biometrika*, *68*(3), 589-599.
847 Elkins, T., & Ganetzky, B. (1990). Conduction in the giant nerve fiber pathway in temperature-
848 sensitive paralytic mutants of Drosophila. *Journal of Neurogenetics*, *6*(4), 207-219.
849 doi:10.3109/01677069009107111
850 Engel, J. E., & Wu, C.-F. (1992). Interactions of membrane excitability mutations affecting
851 potassium and sodium currents in the flight and giant fiber escape systems of Drosophila.
852 *Journal of Comparative Physiology A*, *171*(1), 93-104.
853 Engel, J. E., & Wu, C.-F. (1996). Altered habituation of an identified escape circuit in
854 Drosophila memory mutants. *Journal of Neuroscience*, *16*(10), 3486-3499.
855 Engel, J. E., & Wu, C. F. (1998). Genetic dissection of functional contributions of specific
856 potassium channel subunits in habituation of an escape circuit in Drosophila. *Journal of*
857 *Neuroscience*, *18*(6), 2254-2267. doi:10.1523/jneurosci.18-06-02254.1998
858 Engel, J. E., & Wu, C. F. (2009). Neurogenetic approaches to habituation and dishabituation in
859 Drosophila. *Neurobiology of Learning and Memory*, *92*(2), 166-175.
860 doi:10.1016/j.nlm.2008.08.003
861 Engel, J. E., Xie, X.-J., Sokolowski, M. B., & Wu, C.-F. (2000). A cGMP-dependent protein
862 kinase gene, foraging, modifies habituation-like response decrement of the giant fiber
863 escape circuit in Drosophila. *Learning & Memory*, *7*(5), 341-352.
864 Finkel, T., & Holbrook, N. J. (2000). Oxidants, oxidative stress and the biology of ageing.
865 *Nature*, *408*(6809), 239-247.
866 Frankel, A., & Brousseau, G. (1968). Drosophila medium that does not require dried yeast.
867 *Drosophila Information Service*, *43*, 184.

868 Ganetzky, B., & Wu, C. F. (1982). Indirect Suppression Involving Behavioral Mutants with
869 Altered Nerve Excitability in DROSOPHILA MELANOGASTER. *Genetics, 100*(4),
870 597-614.
871 Gargano, J. W., Martin, I., Bhandari, P., & Grotewiel, M. S. (2005). Rapid iterative negative
872 geotaxis (RING): a new method for assessing age-related locomotor decline in
873 Drosophila. *Experimental Gerontology, 40*(5), 386-395.
874 Gendron, C. M., Kuo, T. H., Harvanek, Z. M., Chung, B. Y., Yew, J. Y., Dierick, H. A., &
875 Pletcher, S. D. (2014). Drosophila life span and physiology are modulated by sexual
876 perception and reward. *Science, 343*(6170), 544-548. doi:10.1126/science.1243339
877 Gorczyca, M., & Hall, J. C. (1984). Identification of a cholinergic synapse in the giant fiber
878 pathway of Drosophila using conditional mutations of acetylcholine synthesis. *Journal of*
879 *Neurogenetics, 1*(4), 289-313.
880 Gordon, S., & Dickinson, M. H. (2006). Role of calcium in the regulation of mechanical power
881 in insect flight. *Proceedings of the National Academy of Sciences of the United States of*
882 *America, 103*(11), 4311-4315. doi:10.1073/pnas.0510109103
883 Götz, K. G. (1968). Flight control in Drosophila by visual perception of motion. *Kybernetik,*
884 *4*(6), 199-208. doi:10.1007/bf00272517
885 Götz, K. G. (1987). Course-control, metabolism and wing interference during ultralong tethered
886 flight in Drosophila melanogaster. *Journal of Experimental Biology, 128*(1), 35-46.
887 Harcombe, E. S., & Wyman, R. J. (1977). Output pattern generation by Drosophila flight
888 motoneurons. *Journal of Neurophysiology, 40*(5), 1066-1077.
889 Harman, D. (1956). Aging: A Theory Based on Free Radical and Radiation Chemistry. *Journal*
890 *of Gerontology, 11*(3), 298-300. doi:10.1093/geronj/11.3.298
891 Harman, D. (1981). The aging process. *Proceedings of the National Academy of Sciences of the*
892 *United States of America, 78*(11), 7124-7128. doi:10.1073/pnas.78.11.7124
893 Hart, P. J., Balbirnie, M. M., Ogihara, N. L., Nersissian, A. M., Weiss, M. S., Valentine, J. S., &
894 Eisenberg, D. (1999). A structure-based mechanism for copper− zinc superoxide
895 dismutase. *Biochemistry, 38*(7), 2167-2178.
896 Harvanek, Z. M., Lyu, Y., Gendron, C. M., Johnson, J. C., Kondo, S., Promislow, D. E. L., &
897 Pletcher, S. D. (2017). Perceptive costs of reproduction drive ageing and physiology in
898 male Drosophila. *Nat Ecol Evol, 1*(6), 152. doi:10.1038/s41559-017-0152
899 Heisenberg, M., & Wolf, R. (1984). Visual Control in Free Flight. In *Vision in Drosophila* (pp.
900 180-182). Berlin: Heidelberg.
901 Holt, G. R., Softky, W. R., Koch, C., & Douglas, R. J. (1996). Comparison of discharge
902 variability in vitro and in vivo in cat visual cortex neurons. *Journal of Neurophysiology,*
903 *75*(5), 1806-1814. doi:10.1152/jn.1996.75.5.1806
904 Hwangbo, D. S., Gershman, B., Tu, M. P., Palmer, M., & Tatar, M. (2004). Drosophila dFOXO
905 controls lifespan and regulates insulin signalling in brain and fat body. *Nature,*
906 *429*(6991), 562-566. doi:10.1038/nature02549
907 Iyengar, A., Ruan, H., & Wu, C.-F. (2010). *Physiological correlates of social interaction-*
908 *mediated lifespan extension in sensory-motor integration of Drosophila Sod mutants.*
909 Paper presented at the Society for Neuroscience Annual Meeting, Washington DC.
910 Iyengar, A., & Wu, C.-F. (2014). Flight and seizure motor patterns in Drosophila mutants:
911 simultaneous acoustic and electrophysiological recordings of wing beats and flight
912 muscle activity. *Journal of Neurogenetics, 28*(3-4), 316-328.

913 Iyengar, A., & Wu, C.-F. (2021). Fly seizure EEG: field potential activity in the Drosophila
914 brain. *Journal of Neurogenetics*, *35*(3), 295-305. doi:10.1080/01677063.2021.1950714
915 Iyengar, A. S. R. (2016). *An integrative analysis of neuronal hyperexcitability, central pattern*
916 *generation and aberrant motor behavior through the lens of Drosophila neurogenetics.*
917 (PhD). University of Iowa, Iowa City.
918 Jacobson, J., Lambert, A. J., Portero-Otín, M., Pamplona, R., Magwere, T., Miwa, S., . . .
919 Partridge, L. (2010). Biomarkers of aging in Drosophila. *Aging Cell*, *9*(4), 466-477.
920 doi:10.1111/j.1474-9726.2010.00573.x
921 Janse, C., Van der Roest, M., & Slob, W. (1986). Age-related decrease in electrical coupling of
922 two identified neurons in the mollusc Lymnaea stagnalis. *Brain Research*, *376*(1), 208-
923 212.
924 Jones, O. R., Scheuerlein, A., Salguero-Gómez, R., Camarda, C. G., Schaible, R., Casper, B. B., .
925 . . Vaupel, J. W. (2014). Diversity of ageing across the tree of life. *Nature*, *505*(7482),
926 169-173. doi:10.1038/nature12789
927 Jung, I., Kim, T. Y., & Kim-Ha, J. (2011). Identification of Drosophila SOD3 and its protective
928 role against phototoxic damage to cells. *FEBS Letters*, *585*(12), 1973-1978.
929 doi:10.1016/j.febslet.2011.05.033
930 Kang, H.-L., Benzer, S., & Min, K.-T. (2002). Life extension in Drosophila by feeding a drug.
931 *Proceedings of the National Academy of Sciences*, *99*(2), 838-843.
932 Kapahi, P., Zid, B. M., Harper, T., Koslover, D., Sapin, V., & Benzer, S. (2004). Regulation of
933 lifespan in Drosophila by modulation of genes in the TOR signaling pathway. *Current*
934 *Biology*, *14*(10), 885-890. doi:10.1016/j.cub.2004.03.059
935 Kasuya, J., Iyengar, A., Chen, H.-L., Lansdon, P., Wu, C.-F., & Kitamoto, T. (2019). Milk-whey
936 diet substantially suppresses seizure-like phenotypes of paraShu, a Drosophila voltage-
937 gated sodium channel mutant. *Journal of Neurogenetics*, *33*(3), 164-178.
938 Katzenberger, R. J., Chtarbanova, S., Rimkus, S. A., Fischer, J. A., Kaur, G., Seppala, J. M., . . .
939 Wassarman, D. A. (2015). Death following traumatic brain injury in Drosophila is
940 associated with intestinal barrier dysfunction. *Elife*, *4*. doi:10.7554/eLife.04790
941 Katzenberger, R. J., Loewen, C. A., Wassarman, D. R., Petersen, A. J., Ganetzky, B., &
942 Wassarman, D. A. (2013). A Drosophila model of closed head traumatic brain injury.
943 *Proceedings of the National Academy of Sciences of the United States of America*,
944 *110*(44), E4152-4159. doi:10.1073/pnas.1316895110
945 Kenyon, C. (2001). A conserved regulatory system for aging. *Cell*, *105*(2), 165-168.
946 King, D. G., & Wyman, R. J. (1980). Anatomy of the giant fibre pathway in Drosophila. I. Three
947 thoracic components of the pathway. *Journal of Neurocytology*, *9*(6), 753-770.
948 doi:10.1007/bf01205017
949 Koh, K., Evans, J. M., Hendricks, J. C., & Sehgal, A. (2006). A Drosophila model for age-
950 associated changes in sleep:wake cycles. *Proceedings of the National Academy of*
951 *Sciences of the United States of America*, *103*(37), 13843-13847.
952 doi:10.1073/pnas.0605903103
953 Kuebler, D., & Tanouye, M. A. (2000). Modifications of seizure susceptibility in Drosophila.
954 *Journal of Neurophysiology*, *83*(2), 998-1009.
955 Kuo, T. H., Yew, J. Y., Fedina, T. Y., Dreisewerd, K., Dierick, H. A., & Pletcher, S. D. (2012).
956 Aging modulates cuticular hydrocarbons and sexual attractiveness in Drosophila
957 melanogaster. *Journal of Experimental Biology*, *215*(Pt 5), 814-821.
958 doi:10.1242/jeb.064980

959 Landis, G. N., Abdueva, D., Skvortsov, D., Yang, J., Rabin, B. E., Carrick, J., . . . Tower, J.
960 (2004). Similar gene expression patterns characterize aging and oxidative stress in
961 Drosophila melanogaster. *Proceedings of the National Academy of Sciences of the United*
962 *States of America, 101*(20), 7663-7668. doi:10.1073/pnas.0307605101
963 Lee, J., Iyengar, A., & Wu, C.-F. (2019). Distinctions among electroconvulsion-and
964 proconvulsant-induced seizure discharges and native motor patterns during flight and
965 grooming: Quantitative spike pattern analysis in Drosophila flight muscles. *Journal of*
966 *Neurogenetics, 33*(2), 125-142.
967 Lee, J., & Wu, C.-F. (2002). Electroconvulsive seizure behavior in Drosophila: analysis of the
968 physiological repertoire underlying a stereotyped action pattern in bang-sensitive
969 mutants. *Journal of Neuroscience, 22*(24), 11065-11079.
970 Lee, J., & Wu, C.-F. (2006). Genetic modifications of seizure susceptibility and expression by
971 altered excitability in Drosophila Na+ and K+ channel mutants. *Journal of*
972 *Neurophysiology, 96*(5), 2465-2478.
973 Leffelaar, D., & Grigliatti, T. (1983). Age-dependent behavior loss in adult Drosophila
974 melanogaster. *Developmental Genetics, 4*(3), 211-227.
975 Lehmann, F. O., & Dickinson, M. H. (1997). The changes in power requirements and muscle
976 efficiency during elevated force production in the fruit fly Drosophila melanogaster.
977 *Journal of Experimental Biology, 200*(Pt 7), 1133-1143.
978 Lehmann, F. O., Skandalis, D. A., & Berthé, R. (2013). Calcium signalling indicates bilateral
979 power balancing in the Drosophila flight muscle during manoeuvring flight. *Journal of*
980 *The Royal Society Interface, 10*(82), 20121050.
981 Lehnert, B. P., Baker, A. E., Gaudry, Q., Chiang, A. S., & Wilson, R. I. (2013). Distinct roles of
982 TRP channels in auditory transduction and amplification in Drosophila. *Neuron, 77*(1),
983 115-128. doi:10.1016/j.neuron.2012.11.030
984 Leppik, I. E., Kelly, K. M., deToledo-Morrell, L., Patrylo, P. R., DeLorenzo, R. J., Mathern, G.
985 W., & White, H. S. (2006). Basic research in epilepsy and aging. *Epilepsy Research, 68*
986 *Suppl 1*, S21-37. doi:10.1016/j.eplepsyres.2005.07.014
987 Levine, J. (1973). Properties of the nervous system controlling flight inDrosophila melanogaster.
988 *Journal of comparative physiology, 84*(2), 129-166.
989 Liang, L., Beaudoin, M., Fritz, M., Fulton, R., & Patel, M. (2007). Kainate-induced seizures,
990 oxidative stress and neuronal loss in aging rats. *Neuroscience, 147*(4), 1114-1118.
991 Loeb, J., & Northrop, J. H. (1917). What Determines the Duration of Life in Metazoa?
992 *Proceedings of the National Academy of Sciences of the United States of America, 3*(5),
993 382-386. doi:10.1073/pnas.3.5.382
994 Mair, W., Goymer, P., Pletcher, S. D., & Partridge, L. (2003). Demography of dietary restriction
995 and death in Drosophila. *Science, 301*(5640), 1731-1733.
996 Martinez, V., Javadi, C., Ngo, E., Ngo, L., Lagow, R., & Zhang, B. (2007). Age-related changes
997 in climbing behavior and neural circuit physiology in Drosophila. *Developmental*
998 *Neurobiology, 67*(6), 778-791.
999 Miller, A.-F. (2012). Superoxide dismutases: ancient enzymes and new insights. *FEBS Letters,*
1000 *586*(5), 585-595.
1001 Miller, A. (1950). The internal anatomy and histology of the imago of Drosophila melanogaster.
1002 In M. Demeric (Ed.), *The Biology of Drosophila* (pp. 421-534). New York: John Wiley
1003 and Sons.

1004 Miller, M. S., Lekkas, P., Braddock, J. M., Farman, G. P., Ballif, B. A., Irving, T. C., . . .
1005 Vigoreaux, J. O. (2008). Aging enhances indirect flight muscle fiber performance yet
1006 decreases flight ability in Drosophila. *Biophysical Journal, 95*(5), 2391-2401.
1007 doi:10.1529/biophysj.108.130005
1008 Min, & Benzer, S. (1997). Spongecake and eggroll: two hereditary diseases in Drosophila
1009 resemble patterns of human brain degeneration. *Current Biology, 7*(11), 885-888.
1010 Miquel, J., Lundgren, P. R., Bensch, K. G., & Atlan, H. (1976). Effects of temperature on the life
1011 span, vitality and fine structure of Drosophila melanogaster. *Mechanisms of Ageing and*
1012 *Development, 5*, 347-370.
1013 Mu, L., Bacon, J. P., Ito, K., & Strausfeld, N. J. (2014). Responses of Drosophila giant
1014 descending neurons to visual and mechanical stimuli. *Journal of Experimental Biology,*
1015 *217*(Pt 12), 2121-2129. doi:10.1242/jeb.099135
1016 Oudes, A. J., Herr, C. M., Olsen, Y., & Fleming, J. E. (1998). Age-dependent accumulation of
1017 advanced glycation end-products in adult Drosophila melanogaster. *Mechanisms of*
1018 *Ageing and Development, 100*(3), 221-229. doi:10.1016/s0047-6374(97)00146-2
1019 Partridge, L., Alic, N., Bjedov, I., & Piper, M. D. (2011). Ageing in Drosophila: the role of the
1020 insulin/Igf and TOR signalling network. *Experimental Gerontology, 46*(5), 376-381.
1021 doi:10.1016/j.exger.2010.09.003
1022 Partridge, L., & Gems, D. (2007). Benchmarks for ageing studies. *Nature, 450*(7167), 165-167.
1023 doi:10.1038/450165a
1024 Partridge, L., Hoffmann, A., & Jones, J. (1987). Male size and mating success in Drosophila
1025 melanogaster and D. pseudoobscura under field conditions. *Animal Behaviour, 35*(2),
1026 468-476.
1027 Pavlidis, P., & Tanouye, M. A. (1995). Seizures and failures in the giant fiber pathway of
1028 Drosophila bang-sensitive paralytic mutants. *Journal of Neuroscience, 15*(8), 5810-5819.
1029 Phillips, J. P., Campbell, S. D., Michaud, D., Charbonneau, M., & Hilliker, A. J. (1989). Null
1030 mutation of copper/zinc superoxide dismutase in Drosophila confers hypersensitivity to
1031 paraquat and reduced longevity. *Proceedings of the National Academy of Sciences, 86*(8),
1032 2761-2765.
1033 Phillips, J. P., Parkes, T. L., & Hilliker, A. J. (2000). Targeted neuronal gene expression and
1034 longevity in Drosophila. *Experimental Gerontology, 35*(9-10), 1157-1164.
1035 doi:10.1016/s0531-5565(00)00117-0
1036 Piazza, N., Gosangi, B., Devilla, S., Arking, R., & Wessells, R. (2009). Exercise-training in
1037 young Drosophila melanogaster reduces age-related decline in mobility and cardiac
1038 performance. *PloS One, 4*(6), e5886. doi:10.1371/journal.pone.0005886
1039 Piper, M. D., & Partridge, L. (2007). Dietary restriction in Drosophila: delayed aging or
1040 experimental artefact? *Plos Genetics, 3*(4), e57. doi:10.1371/journal.pgen.0030057
1041 Pletcher, S. D., Macdonald, S. J., Marguerie, R., Certa, U., Stearns, S. C., Goldstein, D. B., &
1042 Partridge, L. (2002). Genome-wide transcript profiles in aging and calorically restricted
1043 Drosophila melanogaster. *Current Biology, 12*(9), 712-723.
1044 Pringle, J. W. S. (1978). The Croonian Lecture, 1977-Stretch activation of muscle: function and
1045 mechanism. *Proceedings of the Royal Society of London. Series B. Biological Sciences,*
1046 *201*(1143), 107-130.
1047 Rankin, C. H., Abrams, T., Barry, R. J., Bhatnagar, S., Clayton, D. F., Colombo, J., . . .
1048 Thompson, R. F. (2009). Habituation revisited: an updated and revised description of the

behavioral characteristics of habituation. *Neurobiology of Learning and Memory, 92*(2), 135-138. doi:10.1016/j.nlm.2008.09.012

Reenan, R. A., & Rogina, B. (2008). Acquired temperature-sensitive paralysis as a biomarker of declining neuronal function in aging Drosophila. *Aging Cell, 7*(2), 179-186. doi:10.1111/j.1474-9726.2008.00368.x

Rogina, B., Benzer, S., & Helfand, S. L. (1997). Drosophila drop-dead mutations accelerate the time course of age-related markers. *Proceedings of the National Academy of Sciences of the United States of America, 94*(12), 6303-6306. doi:10.1073/pnas.94.12.6303

Ruan, H. (2008). *On Drosophila aging: Lifespan plasticity, social-behavioral influences, and neurophysiological indices*: The University of Iowa.

Ruan, H., & Wu, C.-F. (2009). *Neurophysiological indices of aging in Drosophila: Along the giant-fiber sensory-motor pathway.* Paper presented at the Society for Neuroscience Annual Meeting, Chicago, IL.

Ruan, H., & Wu, C. F. (2008). Social interaction-mediated lifespan extension of Drosophila Cu/Zn superoxide dismutase mutants. *Proceedings of the National Academy of Sciences of the United States of America, 105*(21), 7506-7510. doi:10.1073/pnas.0711127105

Şahin, A., Held, A., Bredvik, K., Major, P., Achilli, T. M., Kerson, A. G., . . . Reenan, R. (2017). Human SOD1 ALS Mutations in a Drosophila Knock-In Model Cause Severe Phenotypes and Reveal Dosage-Sensitive Gain- and Loss-of-Function Components. *Genetics, 205*(2), 707-723. doi:10.1534/genetics.116.190850

Simon, A. F., Liang, D. T., & Krantz, D. E. (2006). Differential decline in behavioral performance of Drosophila melanogaster with age. *Mechanisms of Ageing and Development, 127*(7), 647-651. doi:10.1016/j.mad.2006.02.006

Simon, A. F., Shih, C., Mack, A., & Benzer, S. (2003). Steroid control of longevity in Drosophila melanogaster. *Science, 299*(5611), 1407-1410.

Skorupa, D. A., Dervisefendic, A., Zwiener, J., & Pletcher, S. D. (2008). Dietary composition specifies consumption, obesity, and lifespan in Drosophila melanogaster. *Aging Cell, 7*(4), 478-490. doi:10.1111/j.1474-9726.2008.00400.x

Sofola, O., Kerr, F., Rogers, I., Killick, R., Augustin, H., Gandy, C., . . . Partridge, L. (2010). Inhibition of GSK-3 ameliorates Abeta pathology in an adult-onset Drosophila model of Alzheimer's disease. *Plos Genetics, 6*(9), e1001087. doi:10.1371/journal.pgen.1001087

Sokal, R. R., & Rohlf, F. J. (1969). *Biometry* (4th ed.). New York: W. H. Freeman.

Sudmeier, L. J., Howard, S. P., & Ganetzky, B. (2015). A Drosophila model to investigate the neurotoxic side effects of radiation exposure. *Disease Models & Mechanisms, 8*(7), 669-677.

Sujkowski, A., Bazzell, B., Carpenter, K., Arking, R., & Wessells, R. J. (2015). Endurance exercise and selective breeding for longevity extend Drosophila healthspan by overlapping mechanisms. *Aging, 7*(8), 535-552. doi:10.18632/aging.100789

Tallis, R., Hall, G., Craig, I., & Dean, A. (1991). How common are epileptic seizures in old age? *Age and Ageing, 20*(6), 442-448. doi:10.1093/ageing/20.6.442

Tamura, T., Chiang, A.-S., Ito, N., Liu, H.-P., Horiuchi, J., Tully, T., & Saitoe, M. (2003). Aging specifically impairs amnesiac-dependent memory in Drosophila. *Neuron, 40*(5), 1003-1011.

Tanouye, M. A., & Wyman, R. J. (1980). Motor outputs of giant nerve fiber in Drosophila. *Journal of Neurophysiology, 44*(2), 405-421.

1094 Toivonen, J. M., & Partridge, L. (2009). Endocrine regulation of aging and reproduction in
1095 Drosophila. *Molecular and Cellular Endocrinology, 299*(1), 39-50.
1096 Tower, J. (1996). Aging mechanisms in fruit files. *Bioessays, 18*(10), 799-807.
1097 doi:10.1002/bies.950181006
1098 Tower, J. (2011). Heat shock proteins and Drosophila aging. *Experimental Gerontology, 46*(5),
1099 355-362. doi:10.1016/j.exger.2010.09.002
1100 Trimarchi, J. R., & Schneiderman, A. M. (1995a). Different neural pathways coordinate
1101 Drosophila flight initiations evoked by visual and olfactory stimuli. *Journal of*
1102 *Experimental Biology, 198*(Pt 5), 1099-1104.
1103 Trimarchi, J. R., & Schneiderman, A. M. (1995b). Flight initiations in Drosophila melanogaster
1104 are mediated by several distinct motor patterns. *Journal of Comparative Physiology. A:*
1105 *Sensory, Neural, and Behavioral Physiology, 176*(3), 355-364. doi:10.1007/bf00219061
1106 Trout, W. E., & Kaplan, W. D. (1970). A relation between longevity, metabolic rate, and activity
1107 in shaker mutants of Drosophila melanogaster. *Experimental Gerontology, 5*(1), 83-92.
1108 doi:10.1016/0531-5565(70)90033-1
1109 Ueda, A., Iyengar, A., & Wu, C.-F. (2021). Differential effects on neuromuscular physiology
1110 between Sod1 loss-of-function mutation and paraquat-induced oxidative stress in
1111 Drosophila. *microPublication biology, 2021*, 10.17912/micropub.biology.000385.
1112 doi:10.17912/micropub.biology.000385
1113 Ueda, A., Woods, S., McElree, I., O'Harrow, T. C., Inman, C., Thenuwara, S., . . . Iyengar, A.
1114 (2018). Two novel forms of ERG oscillation in Drosophila: age and activity dependence.
1115 *Journal of Neurogenetics, 32*(2), 118-126.
1116 Vaupel, J. W., Carey, J. R., Christensen, K., Johnson, T. E., Yashin, A. I., Holm, N. V., . . .
1117 Curtsinger, J. W. (1998). Biodemographic trajectories of longevity. *Science, 280*(5365),
1118 855-860. doi:10.1126/science.280.5365.855
1119 von Reyn, C. R., Nern, A., Williamson, W. R., Breads, P., Wu, M., Namiki, S., & Card, G. M.
1120 (2017). Feature Integration Drives Probabilistic Behavior in the Drosophila Escape
1121 Response. *Neuron, 94*(6), 1190-1204.e1196. doi:10.1016/j.neuron.2017.05.036
1122 Woods, S. A. (2017). *Behavioral and physiological effects of oxidative stress throughout the*
1123 *lifecycle of Drosophila sod1 mutants.* (MS). University of Iowa, Iowa City.
1124 Wu, C.-F., & Ruan, H. (2008). *Social interaction-mediated lifespan extension and*
1125 *electrophysiological correlates in Drosophila Cu/Zn superoxide dismutase mutants.*
1126 Paper presented at the Society for Neuroscience Annual Meeting, Washington DC.
1127 Yamazaki, D., Horiuchi, J., Nakagami, Y., Nagano, S., Tamura, T., & Saitoe, M. (2007). The
1128 Drosophila DCO mutation suppresses age-related memory impairment without affecting
1129 lifespan. *Nature Neuroscience, 10*(4), 478-484.
1130 Yeoman, M., & Faragher, R. (2001). Ageing and the nervous system: insights from studies on
1131 invertebrates. *Biogerontology, 2*(2), 85-97.
1132 Zhao, X. L., Wang, W. A., Tan, J. X., Huang, J. K., Zhang, X., Zhang, B. Z., . . . Huang, F. D.
1133 (2010). Expression of beta-amyloid induced age-dependent presynaptic and axonal
1134 changes in Drosophila. *Journal of Neuroscience, 30*(4), 1512-1522.
1135 doi:10.1523/jneurosci.3699-09.2010
1136 Ziegler, D. V., Wiley, C. D., & Velarde, M. C. (2015). Mitochondrial effectors of cellular
1137 senescence: beyond the free radical theory of aging. *Aging Cell, 14*(1), 1-7.

1138

Table 1. Features of GF Pathway SLR and LLR in young and aged flies

			WT 25 °C				WT 29 °C				*Sod* 23 °C			
		% Mort.	<1	5	50	95	<1	5	50	95	<1	5	50	95
GF Short-Latency Response Properties	Threshold	N (flies)	9	8	9	10	13	10	9	9	9	9	9	10
		Mean (V)	10.1	10.2	9.9	9.9	9.0	8.6	12.1	10.0	12.9	10.8	9.9	9.8
		S.D. (V)	1.9	3.1	1.7	3.7	2.6	2.1	4.7	2.5	5.0	3.9	2.9	4.5
		C.V.	0.19	0.30	0.17	0.37	0.29	0.24	0.39	0.25	0.39	0.36	0.29	0.46
	Latency	N (flies)	9	8	9	10	13	12	11	9	10	9	9	10
		Mean (ms)	1.1	1.5	1.3	1.4	1.3	1.4	1.4	1.3	1.6	1.5	1.3	1.2
		S.D. (ms)	0.3	0.2	0.2	0.3	0.3	0.3	0.3	0.5	0.2	0.3	0.3	0.2
		C.V.	0.27	0.13	0.15	0.21	0.23	0.21	0.21	0.38	0.13	0.20	0.23	0.17
	R.P.	N (flies)	9	8	9	10	10	9	9	8	9	7	9	10
		Mean (ms)	3.8	4.6	4.3	5.1	3.8	4.7	6.0	7.1	9.2	4.1	3.7	5.3
		S.D. (ms)	1.0	1.8	1.6	3.5	0.9	1.9	1.4	8.3	8.0	2.3	1.5	2.5
		C.V.	0.26	0.39	0.37	0.69	0.24	0.40	0.23	1.17	0.87	0.56	0.41	0.47
	Resp. 30 P.	N (flies)	9	8	9	10	10	8	9	8	9	8	8	10
		Mean (resp.)	18.9	19.4	16.8	15.6	18.4	20.0	14.3	12.6	5.9	9.3	8.9	10.7
		S.D. (resp.)	4.6	5.2	6.9	8.1	7.3	9.8	10.7	9.4	3.6	4.5	6.4	7.6
		C.V.	0.24	0.27	0.41	0.52	0.40	0.49	0.75	0.75	0.61	0.48	0.72	0.71
GF Long-Latency Response Properties	Threshold	N (flies)	13	14	18	12	12	13	14	12	14	17	11	11
		Mean (V)	3.6	3.3	3.9	4.6	3.5	4.1	4.6	4.9	4.4	4.2	4.7	5.2
		S.D. (V)	0.8	0.7	1.2	2.0	0.6	1.1	1.4	0.6	1.0	1.5	1.5	1.0
		C.V.	0.22	0.21	0.31	0.43	0.17	0.27	0.30	0.12	0.23	0.36	0.32	0.19
	Latency	N (flies)	13	14	18	12	12	13	14	12	14	17	11	11
		Mean (ms)	4.1	4.3	4.3	4.5	4.3	4.4	4.7	4.8	4.5	4.2	4.4	4.3
		S.D. (ms)	0.4	0.3	0.2	0.3	0.4	0.3	0.4	0.5	0.5	0.5	0.7	0.5
		C.V.	0.10	0.07	0.05	0.07	0.09	0.07	0.09	0.10	0.11	0.12	0.16	0.12
	R.P.	N (flies)	13	14	18	12	12	13	14	12	14	17	11	11
		Mean (ms)	41.2	45.4	38.3	87.9	67.5	49.2	145.9	162.5	106.1	71.5	89.0	120.9
		S.D. (ms)	22.2	43.5	18.5	90.8	35.6	23.9	123.5	165.9	68.1	24.9	66.6	66.3
		C.V.	0.54	0.96	0.48	1.03	0.53	0.49	0.85	1.02	0.64	0.35	0.75	0.55

1140

1141

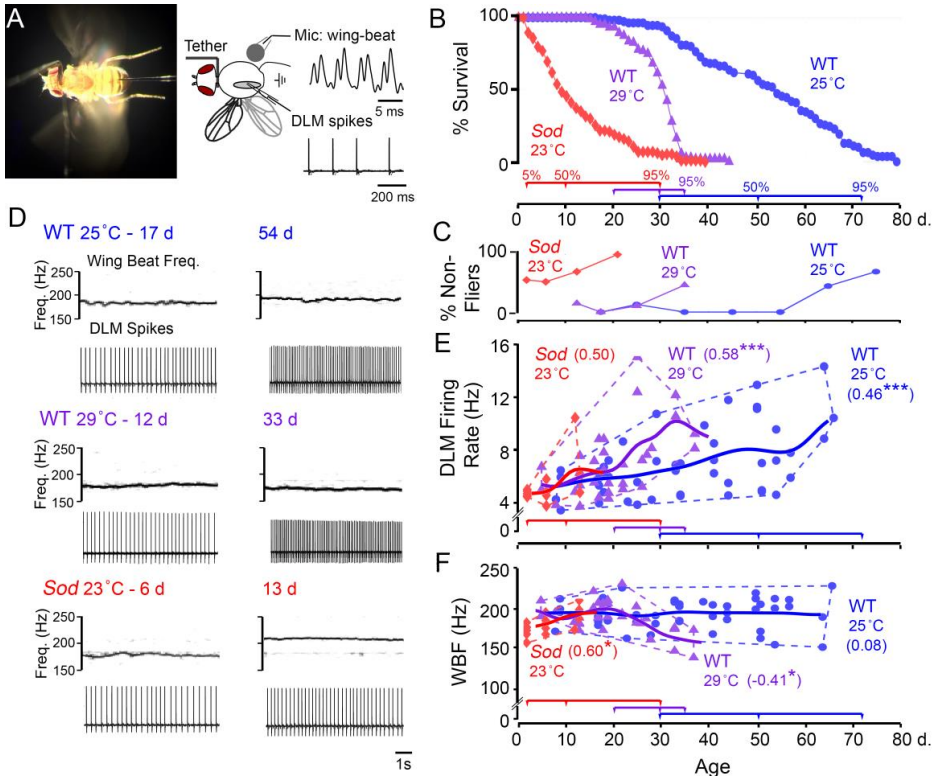

Figure 1. Flight motor performance across the lifespan of WT control and *Sod* mutant flies. (A, Left) Photograph of tethered fly preparation used in the flight and electrophysiological assays. Spiking activity in the DLM was monitored by a tungsten microelectrode, and acoustic signals generated by wing beats were picked up via a microphone placed below the fly. (Right) A schematic drawing of the preparation and sample waveforms of the respective signals. (B) Lifespan curves of WT flies (reared at 25 ˚C, blue circles, n = 110; and 29 ˚C, purple triangles, n = 104), and *Sod* mutants (red diamonds, reared at 23 ˚C, n = 134). Colored timelines below indicate the ages corresponding to 5%, 50% and 95% mortality for the respective curves. See Extended Data Figure 1-1 for log-transformed mortality curves. (C) The proportion of non-fliers (see Methods for definition) across the lifespan (n > 10 for each point). (D) Representative spectrograms of the microphone signal (upper panels) indicating the wing beat frequency (WBF) and corresponding traces of DLM spiking (lower panels) during sustained flight in younger (left column) and aged flies (right column) from the populations tested. (E-F) Scatterplots of the DLM firing rate (E) and WBF (F) during sustained flight in 25 ˚C- and 29 ˚C-reared WT flies (blue circles and purple triangles respectively), and in *Sod* mutants (red diamonds). Trend lines represent a Gaussian-kernel running average of the age-trajectory for the three populations (kernel window sizes of 10, 6 and 6 d respectively). The age-dependent Spearman's rank correlation coefficient (r_s) is indicated for each population (n = 48, 33, and 15 flies for WT 25 ˚C-, WT 29 ˚C-reared and *Sod* respectively). For this and following figures, * $p < 0.05$, ** $p < 0.01$, *** $p < 0.001$.

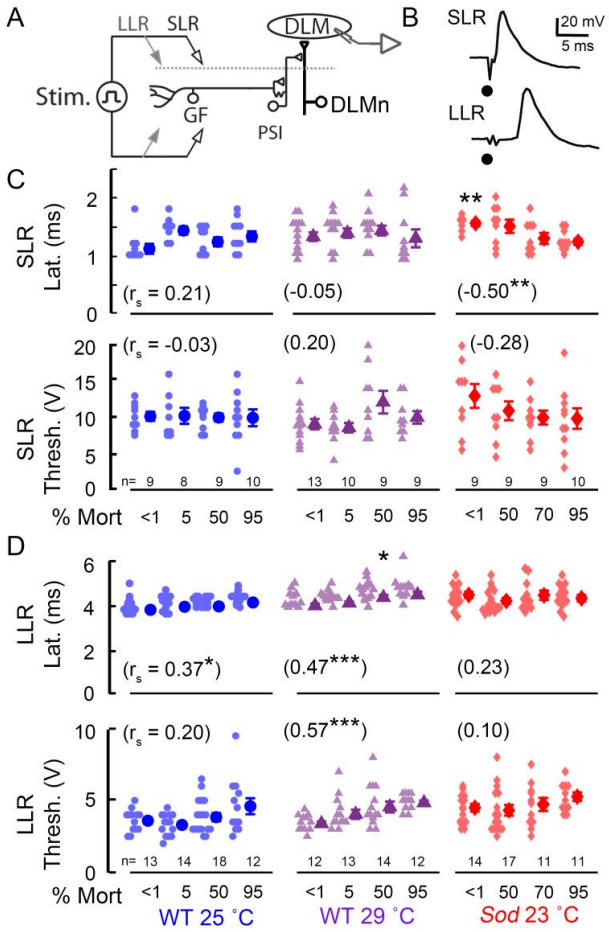

Figure 2. Performance characteristics of the GF pathway and its afferent inputs in aged WT and *Sod* mutant flies.

(A) Overview of the GF "jump-and-flight" escape pathway. The GF neuron activates the indirect flight muscle DLM through a peripherally-synapsing interneuron (PSI) which innervates the DLM motor neuron (DLMn). For clarity, the GF branch that directly innervates the jump muscle (TTM) is not shown. (B) Electrical stimulation across the brain activates the GF pathway, and motor output is monitored via DLM action potentials in the tethered fly. High-intensity stimuli directly activate the GF neuron, giving rise to short-latency responses (SLRs). Lower-intensity stimuli recruit GF afferent inputs, resulting in the DLM long-latency responses (LLRs). Dots indicate stimulus artifact. (C-D) SLR and LLR latency and threshold across the lifespan of WT and *Sod* flies. In this figure and in Figures 3 and 5, mean and SEM are indicated to the right of each dataset. Each lighter colored data point represents measurement from a single fly. Asterisks indicate significant difference against mortality-matched, 25 ℃-reared WT flies (Kruskal-Wallis ANOVA, rank-sum *post hoc* test). The numbers in parenthesis indicate Spearman correlation coefficient (r_s) of the parameter measurements vs. age categories.

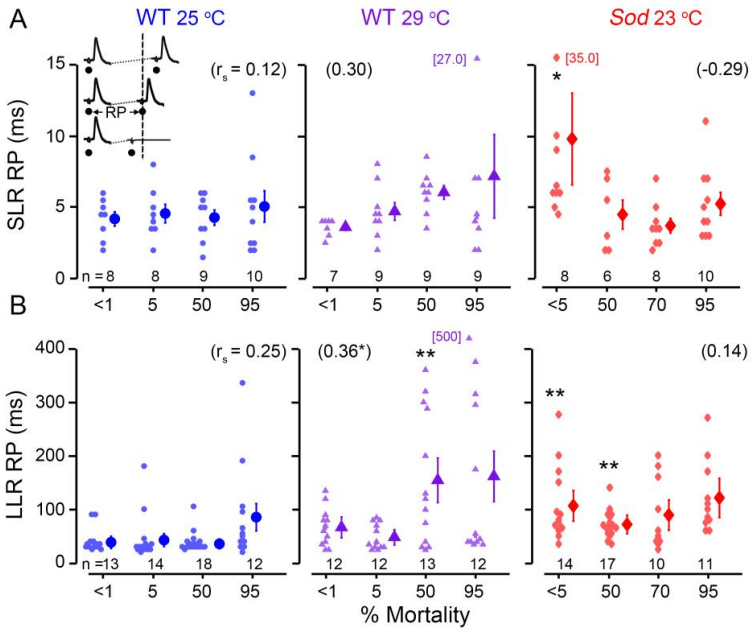

Figure 3. Paired-pulse refractory characteristics of GF-mediated DLM short- and long-latency responses.

The paired-pulse refractory period (RP) represents the shortest inter-stimulus interval where the second stimulus evokes a DLM spike; shorter stimulus intervals fail to recruit two spikes (inset). (A-B) Scatter plots of the SLR (A) and LLR (B) RPs from WT flies reared at 25 ˚C and 29 ˚C as well as *Sod* flies reared at 23 ˚C are shown over the course of their lifespans, presented as percent mortality. Outlier values exceeding the axis range are indicated adjacently. See Figure 2 legend for statistical treatment and presentation. Data from the related SLR following frequency (FF_{30}) protocol is shown in Extended Data Figure 3-1.

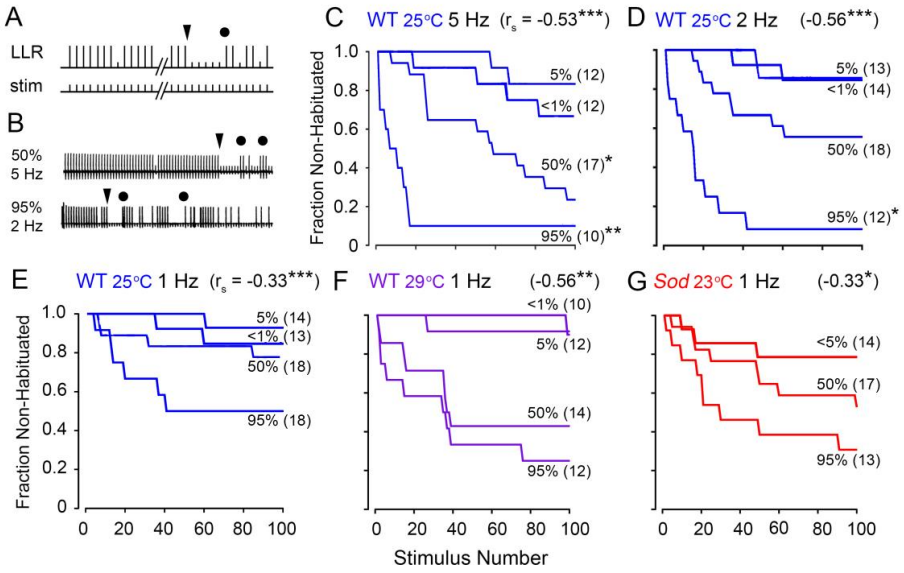

Figure 4. Age-dependent alterations in habituation kinetics of GF afferents.
(A) Habituation of GF afferents. Habituation is operationally defined as the first instant of reaching five-consecutive DLM spike failures to LLR-evoking stimulation train of defined frequency (triangle, cf. Engel & Wu, 1996). Subsequent dis-habituation stimulus (circle, air puff) triggered recovery of LLRs, excluding sensory adaptation or motor fatigue as the basis for DLM response failure. (B) Sample traces from WT flies reared at 25 ˚C of slower habituation at 50 % mortality (upper trace, 5 Hz stimulation) and faster habituation at 95% mortality (lower trace, 2 Hz stimulation). (C-E) Frequency dependence of LLR habituation in 25 ˚C-reared WT flies to stimulation at 5 Hz (C), 2 Hz (D), and 1 Hz (E). The fraction of flies in the sample population of each age group (<1, 5, 50, 95% mortality) that were not habituated after a given number of stimuli is plotted. (F-G) Habituation in WT 29 °C-reared flies (F) and in *Sod* mutants (G) to 1 Hz stimulation. Sample sizes as indicated next to each plot. Asterisks at the end of the trace indicate significantly faster habituation compared to habituation in mortality-matched WT 25 ˚C-reared flies to 1 Hz stimulation (log-rank test). The age-dependent Spearman correlation coefficient (r_s) is indicated in the upper-right corners of each panel.

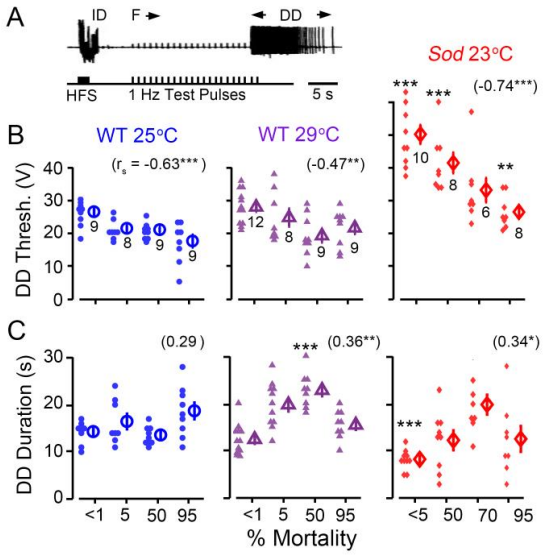

Figure 5. Decreasing threshold of electroconvulsive seizure (ECS) discharges in aging flies. (A) ECS activity was evoked by a short train (2 s) of high intensity, high frequency stimulation (0.1 ms pulse duration, 200 Hz, HFS) across the head in tethered flies. DLM spike discharges serve as a convenient monitor of these seizures, and the pattern of these discharges is highly stereotypic (cf. Lee & Wu, 2002), consisting of an initial spike discharge (ID), followed by a period of paralysis corresponding to failure of test pulse-evoked GF pathway responses (F), and a delayed spike discharge (DD). The example trace here shows the sequence in a young 25 ˚C-reared WT fly. (B-C) Scatterplots of the stimulation threshold to induce DD (B), and duration of the evoked DD (C) across the lifespans of 25 ˚C- and 29 ˚C-reared WT and *Sod* mutants. Mean and SEM are indicated to the right of each group, sample sizes below. See Figure 2 legend for other details of statistical treatment and presentation. See Extended Data Figure 5-1 for analysis of spiking during the DD.

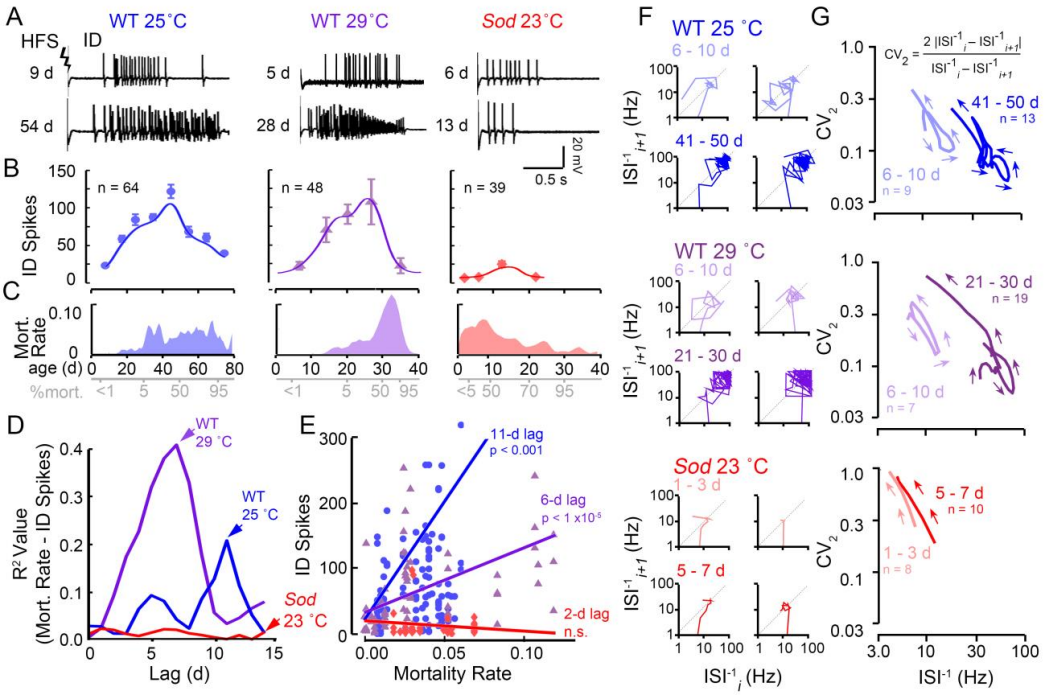

Figure 6. Age-dependent alterations in ID spike counts vs mortality rates and signatures of ID spiking trajectories in WT and *Sod* flies.

(A) Representative high frequency stimulation-induced IDs from young (< 1 % mortality; 9, 5 and 6 d traces) and aged (50% mortality; 54, 28 and 13 d traces) WT and *Sod* flies (stimulation voltage: 80 V). (B) Plot of the number of spikes within the ID across the lifespan (mean ± SEM for different age groups, and sample sizes across the populations are indicated). Trend lines represent a Gaussian-kernel running average (see Figure 1) of the age-trajectory for the three populations. (C) Plot of the mortality rates (defined as the negative slope of the lifespan curve, Figure 1B) across the lifespan for the three populations examined (see Extended Data Figure 1-1 for log-transformed mortality rate plots). (D) Linear cross-correlation between the mortality rate and ID spike count upon introducing a lag of 0 – 15 days to determine the optimal lag for maximal correlation, i.e. 11 and 6 d for 25 °C and 29 °C -reared WT flies. In *Sod* mutants no significant correlation between mortality rate and ID spike count was detected. (E) Plot of best correlation between of lagged ID spike count versus mortality rate for the three populations. (p-values as indicated). (F) Poincaré plots of representative IDs from young (< 1% mortality) and aged (~50% mortality) flies. The instantaneous firing frequency of each inter-spike interval (ISI^{-1}_{i}) is plotted against the next spike interval (ISI^{-1}_{i+1}) on a log scale (see text). (G) Averaged trajectories (as constructed in Lee et al., 2019) of the inter-spike interval (ISI^{-1}) versus the instantaneous coefficient of variation (CV_2, as defined by Holt et al., 1996, see text). Lower values of CV_2 indicate more rhythmic firing. Number of trajectories used to construct the average is as indicated. Note the similar changes in aged 25 °C and 29 °C –reared WT flies compared to young counterparts and distinctions between WT and *Sod* mutant discharges.

1241

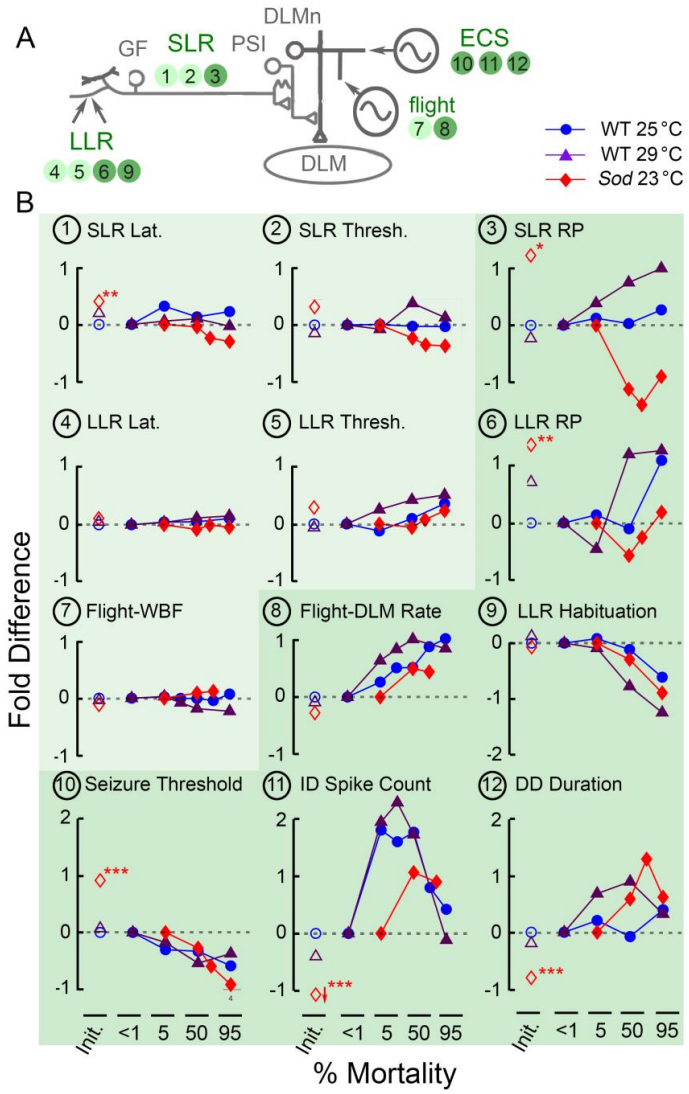

1242
1243 **Figure 7. Distinct age-trajectories of different motor circuit properties examined in this**
1244 **study.**
1245 (A) Schematic diagram of the circuit components generating motor patterns driving DLM
1246 activity examined in this study. Corresponding parameters displayed in panels in (B) are
1247 indicated by corresponding panel numbers. Darker backgrounds indicate that significant age-
1248 dependent alterations were detected. (B) Normalized changes in neurophysiological parameters
1249 of the respective motor circuits are plotted as function of % mortality. Changes are presented in
1250 terms of 'fold change' from the initial (<1% mortality) value (i.e., $\log_2$ [value/initial value]), such
1251 that +1 indicates doubling, while -1 indicates halving of the parameter's value. First, the plot at
1252 the origin (open symbols, <1% mortality) indicate fold changes compared to young WT 25 ˚C

for WT 29 ˚C and *Sod* 23 ˚C young flies. Second, the age-trajectories comparing flies of different ages to the youngest flies are indicate in fold changes (filled symbols: blue, purple and red for WT 25 ˚C, WT 29 ˚C, and *Sod* 23 ˚C respectively). Panels representing circuit parameters that remain relatively robust across the lifespan in all three populations are shaded in lightly shaded, while parameters that display clear age-dependent alterations in at least one rearing condition are shaded darker.

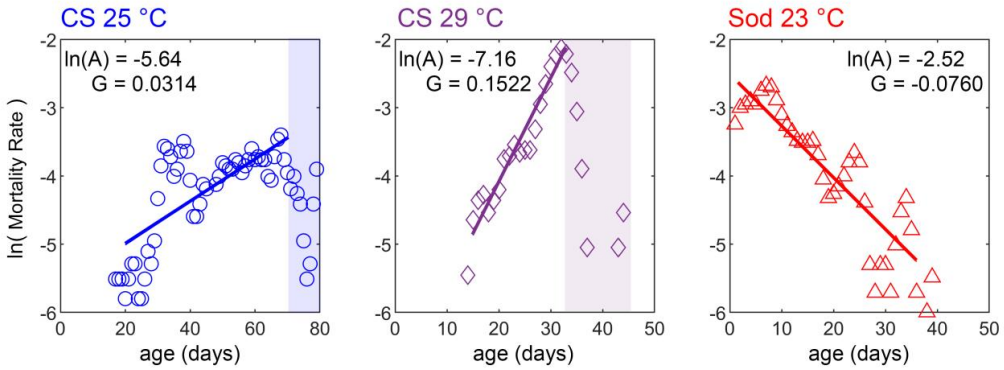

Extended Data Figure 1-1. Log-transformed mortality rate.
The mortality rate is defined as the negative slope of the survival curve (S) [i.e. mortality rate = $-1(S(t_0)-S(t_1))/(t_0-t_1)$, for the interval between time points t_0 and t_1]. The log-transformed mortality rates corresponding to the survival curves in Figure 1B are plotted. Solid lines correspond to the linear Gompertz fit of the mortality rate distribution (i.e. *ln* (mortality rate) = *ln* (*A*) + *Gt*). The fit parameters *A* and *G* for each distribution are indicated. For CS 25 °C and 29 °C-reared flies, the Gompertz line is a reasonable fit for the mortality rate over most of the survival curve. However, there is a marked deviation observed in the oldest flies (~95% survival, shaded region). The *Sod* lifespan curve displays a distinctive negative mortality rate slope implying a potentially distinct set of factors which contribute to mortality in these individuals.

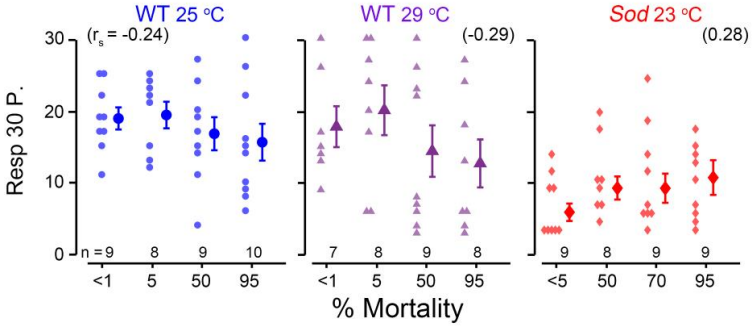

Extended Data Figure 3-1. Giant-fiber SLR properties across the lifespan: FF_{30} protocol. The FF_{30} protocol measures the ability of the GF pathway to follow high-frequency stimulation. Three trains 10 stimuli are delivered at 200 Hz with a 10 s interval between trains (30 total stimuli). The number of responses was recorded (Resp 30 P.), with a higher response rate corresponding to a better ability to follow high-frequency stimulation. Sample sizes as indicated for each age group, and the Spearman rank correlation (r_s) is shown above. No population displayed statistical significance age-dependent trend (i.e. $p > 0.05$).

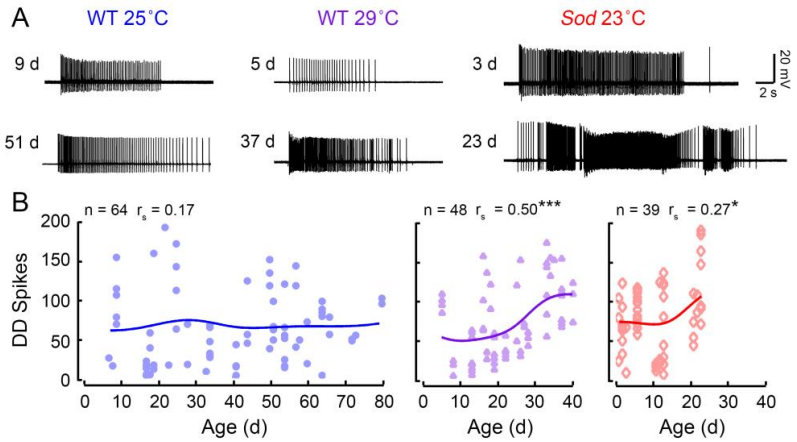

1280 **Extended Data Figure 5-1. DD spiking across the lifespan.** (A) Example traces of DD spiking
1281 in young (top row) and aged (bottom row) flies. (B) Scatterplot of the spike count during the DD.
1282 Trend-line indicates the Gaussian kernel running average as computed in Figure 1. The sample
1283 size and age-dependent rank correlation (r_s) are indicated above. (* $p < 0.05$, *** $p < 0.001$).
1284